

EHF for Satellite Communications: the New Broadband Frontier

By ERNESTINA CIANCA, *MEMBER IEEE*, TOMMASO ROSSI, ASHER YAHALOM, YOSEF PINHASI, JOHN FARSEROTU, *SENIOR MEMBER IEEE* AND CLAUDIO SACCHI, *SENIOR MEMBER IEEE*

ABSTRACT: the exploitation of Extremely High Frequency (EHF) bands (30-300 GHz) for broadband transmission over satellite links is a hot research topic nowadays. In particular, the Q-V band (30-50 GHz) and W-band (75-110 GHz) seem to offer very promising perspectives. This paper aims at presenting an overview of the current status of research and technology in EHF satellite communications and taking a look at future perspectives in terms of applications and services. Challenges and open issues are adequately considered together with some viable solutions and future developments. The proposed analysis highlighted the need for a reliable propagation model based on experimental data acquired in orbit. Other critical aspects should be faced at the PHY-layer level in order to manage the tradeoff between power efficiency, spectral efficiency and robustness against link distortions. As far as networking aspects are concerned, the large bandwidth availability should be converted into increased throughput by means of suitable radio resource management and transport protocols, able to support very high data-rates in long-range aerospace scenarios.

KEYWORDS: Satellite Communications, EHF, Satellite Networking.

1. INTRODUCTION

In the perspective of reaching global and ubiquitous wireless connectivity, the satellite segment will play a key role. The claimed objective is to reach so-called "gigabit connectivity" in order to make the satellite segment a potential "backbone in the air" for next-

generation digital communication services, characterized by high-speed and stringent quality-of-service (QoS) requirements [1]. Such an ambitious objective is not realistically achievable by exploiting currently saturated bandwidth portions (Ku and Ka bands). For this reason, the push towards higher frequencies will characterize future R&D on satellite communications [2]. The prophetic consideration of W.E. Morrow, reported in the issue scanning of *Proceedings of the IEEE* of 2/71 dedicated to Satellite Communications [3] is worth mentioning here. Introducing ref. [4], published in that issue, Morrow claimed: "These research results are of great significance because they indicate the possibilities and limitations of operation to mobile terminals at longer wavelengths and to fixed terminals at millimeter wavelengths. The question of operation at millimeter wavelength is especially important because of the shortage of frequencies in the centimeter wavelength band. If economic millimeter wavelength communication systems can be designed, the total available bandwidth for satellite communications can be increased manyfold."

The millimeter wave domain is also known as the *Extremely High Frequency* (EHF) spectrum range. EHF ranges from 30 GHz to 300 GHz. Early works on atmospheric propagation in EHF [4][5][6] evidenced some favorable and not-favorable frequency bands for future usage for satellite communications. For instance, frequencies around the 60 GHz band cannot be effectively exploited for aerospace transmission because of an Oxygen multiple absorption peaks. On the other hand, the W-band (75-110 GHz) seems to provide a favorable "attenuation window" related to Oxygen absorption. As far as water absorption (clouds, rain) is concerned, a local minimum is encountered at 35 GHz. Then, H₂O attenuation almost linearly increases with

Ernestina Cianca and Tommaso Rossi are with the University of Rome "Tor Vergata", Department of Electronic Engineering, Via del Politecnico 1, 00133 Rome, Italy (e-mail: tommaso.rossi@uniroma2.it, ernestina.cianca@uniroma2.it)

Asher Yahalom and Josef Pinhasi are with the Ariel University Center of Samaria, Department of Electrical and Electronic Engineering, P.O. Box 3, Ariel 40700, Israel (e-mail: asya@ariel.ac.il, yosip@ariel.ac.il)

John Farserotu is with Centre Suisse d'Electronique et de Microtechnique (CSEM), Zurich (CH) (e-mail: john.farserotu@csem.ch)

Claudio Sacchi is with the University of Trento Department of Information Engineering and Computer Science (DISI), Via Sommarive 5, I-38123, Trento, Italy (e-mail: sacchi@disi.unitn.it)

frequency until 100 GHz and reaches a huge peak around 180 GHz. From these considerations, it is possible to individuate some favorable EHF bandwidth portions exploitable for satellite communications, i.e.: the Q-V band (30-50 GHz) and the already mentioned W-band. Research and experimental studies about satellite communications in EHF are mainly focused on the utilization of these two bands. The exploitation of EHF may offer many theoretical advantages for wireless communications, which make it suitable for satellite links, i.e. [7]:

- Broad bandwidths for high data rate information transfer;
- High directivity and spatial resolution;
- Low transmission power (due to high antenna gain);
- Low probability of interference/ interception (due to narrow antenna beam-widths);
- Small antenna and equipment size;
- Reduced size of satellite and launch vehicles.

The main disadvantages of satellite communications at EHF arise from the increased free-space path loss, the increased water vapor absorption and rain fading as well as the low efficiency and relatively low power available from currently available sources. For the higher part of the EHF spectrum, such as the W-band, no realistic model is given for the effects of clouds, gases and atmospheric precipitations. Moreover, physical layer issues, such as: phase noise, carrier recovery in the presence of large Doppler shifts and nonlinear distortions require deep investigations and involve stringent requirements on the baseband modem section.

This paper aims at establishing a landmark of the state-of-the-art of EHF satellite communications, dealing with open issues related to signal propagation, physical layer constraints and showing to readers some proposed solutions in terms of modulation, coding, power allocation, pulse shaping, etc., considering future research trends in the field. However, the paper does not only address physical layer aspects. It also deals with the practical utilization of the EHF band in order to provide final users with specific broadband services of commercial and social interest. An overview of current and future experiments concerning satellite EHF transmission is also provided, in order to make readers aware of the intensive R&D activities involving the coordinated efforts of national and international Space Agencies and Space Industries.

The paper is structured as follows: Section 2 considers the EHF channel propagation aspects in the framework of satellite communications. Section 3 deals with those link impairments typical of high-frequency satellite communications, which are inherent to the non-ideal behavior of transmission devices. Section 4 shows some feasible PHY-layer solutions targeted at

reaching the most efficient exploitation of the available bandwidth resources. Section 5 focuses on networking and application aspects. Section 6 provides a summary of the most relevant planned and operative EHF satellite missions, together with a look at operational systems "beyond Ka-band". Finally, conclusions are drawn in Section 7.

2. EHF SATELLITE CHANNEL PROPAGATION

A. Atmospheric propagation of EHF waves

Some of the principal challenges in realizing modern wireless communication links at the EHF band are the effects emerging when the electromagnetic radiation propagates through the atmosphere. When millimeter-wave radiation passes through the atmosphere, it suffers from selective molecular absorption [8]. Several empirical and analytical models were suggested for estimating the millimeter and infrared wave transmission of the atmospheric medium. The transmission characteristics of the atmosphere at the EHF band, as shown in Fig. 1, was calculated with the millimeter propagation model (MPM), developed by Liebe [9-12]. Curves are drawn for several values of relative-humidity (RH), assuming clear sky and no rain. Inspection of Fig. 1 reveals absorption peaks at 22GHz and 183GHz, where resonance absorption of water (H_2O) occurs, as well as absorption peaks at 60GHz and 119GHz, due to absorption resonances of oxygen (O_2). Between these frequencies, minimum attenuation is obtained at 35GHz (Ka-band), 94GHz (W-band), 130GHz and 220GHz, which are known as atmospheric transmission 'windows' [6]. The inhomogeneous transmission in a band of frequencies causes absorptive and dispersive effects in amplitude and phase of wide-band signals transmitted in the EHF band [13-15]. The frequency response of the atmosphere plays a significant role as the data rate of a wireless digital radio channel is increased. The resulting amplitude and phase distortion leads to inter-symbol interference and thus to an increase in the bit error rate (BER). These effects must be taken into account in the design of broadband communication systems, including careful consideration of appropriate modulation, equalization and multiplexing techniques.

The time dependent field $E(t)$ represents an electromagnetic wave propagating in a medium. The Fourier transform of the field is:

$$\mathbf{E}(jf) = \int_{-\infty}^{+\infty} \mathbf{E}(t) \cdot e^{-j2\pi ft} dt \quad (1)$$

In the far field, transmission of a wave, radiated from a localized (point) isotropic source and propagating in a

medium to a distance d is characterized in the frequency domain by the approximate transfer function:

$$H(jf) = \frac{\mathbf{E}_{out}(jf, d)}{\mathbf{E}_{in}(jf)} \propto \frac{1}{d} \cdot e^{-j \int_0^d k(f) dz} \quad (2)$$

Here, $k(f) = 2\pi f \sqrt{\mu \epsilon}$ is a frequency dependent propagation factor, where ϵ and μ are the local permittivity and the permeability of the medium, respectively. The transfer function $H(jf, d)$ describes the frequency response of the medium. In a dielectric medium the permeability is equal to that of vacuum $\mu = \mu_0$ and the permittivity is given by $\epsilon(f) = \epsilon_r(f) \cdot \epsilon_0$. If the medium introduces losses and dispersion, the relative dielectric constant $\epsilon_r(f)$ is a complex, frequency dependent function. The resulting local index of refraction can be presented by [14-15]:

$$n(f) = \sqrt{\epsilon_r(f)} = 1 + N(f) \cdot 10^{-6} \quad (3)$$

Where $N(f) = N_0 + N'(f) - jN''(f)$ is the complex refractivity given in MPM [11]. The propagation factor can be written in terms of the index of refraction:

$$k(f) = \frac{2\pi f}{c} \cdot n(f) = -j \underbrace{\frac{2\pi f}{c} \cdot N''(f) \cdot 10^{-6}}_{\alpha(f)} + \underbrace{\frac{2\pi f}{c} \cdot (1 + N_0 \cdot 10^{-6}) + \frac{2\pi f}{c} \cdot N'(f) \cdot 10^{-6}}_{\beta(f)} \quad (4)$$

As shown in Fig.1, the impact of $\Delta\beta(f)$ on the refraction index is small for frequencies lower than 100 GHz (Q/V and W bands). Assuming that a carrier wave at f_c is modulated by a wide-band signal $A_{in}(t)$:

$$E_{in}(t) = \text{Re}\{A_{in}(t) \cdot e^{j2\pi f_c t}\} \quad (5)$$

Here $A_{in}(t) = I_{in}(t) - jQ_{in}(t)$ is a complex envelope, representing the base-band signal, where $I_{in}(t) = \text{Re}\{A_{in}(t)\}$ and $Q_{in}(t) = -\text{Im}\{A_{in}(t)\}$ are the in-phase and the quadrature information waveforms respectively. The complex amplitude after propagation in the medium with the transfer function at distance d $H(jf)$ is calculated by [9]:

$$A_{out}(t) = \int_{-\infty}^{+\infty} \mathbf{A}_{in}(f) \cdot H(f + f_c) \cdot e^{+j2\pi f t} df \quad (6)$$

where $\mathbf{A}_{in}(f)$ is the Fourier transform of $A_{in}(t)$.

Most of the attenuation is accumulated in the troposphere, which is the lowest portion of Earth's atmosphere, containing approximately 75% of the atmosphere's mass and 99% of its water vapor and aerosols. Fig. 2.b shows the accumulated attenuation at 94GHz. It can be shown that most of the attenuation is caused by the lowest 5-6Km layer of the troposphere, depending on humidity. In the worst cases it accumulates about 3.5 dB loss in addition to the free space loss present. For all practical purposes this should be taken as an upper limit for vertical losses.

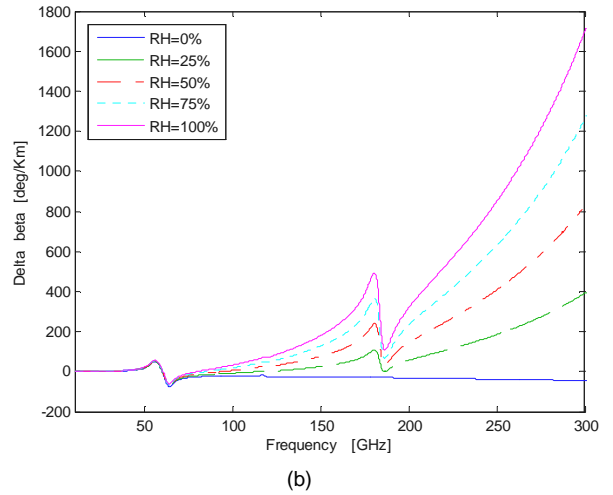
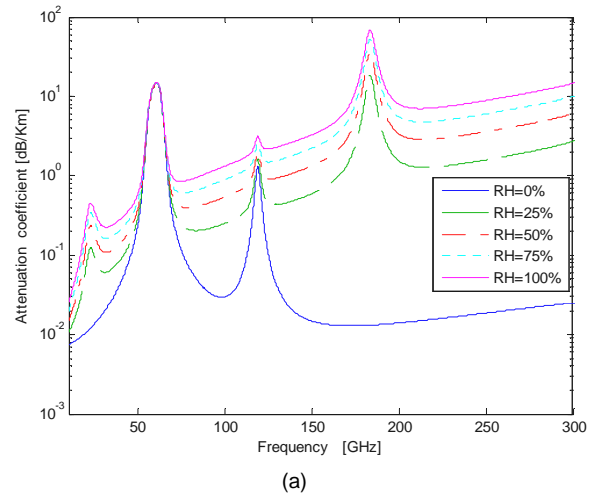


Fig. 1. Millimeter wave a) attenuation coefficient $20 \log(e) \cdot \alpha(f)$ in [dB/Km] and b) $\Delta\beta(f)$ in [deg/Km] for various values of relative humidity (RH) at sea level.

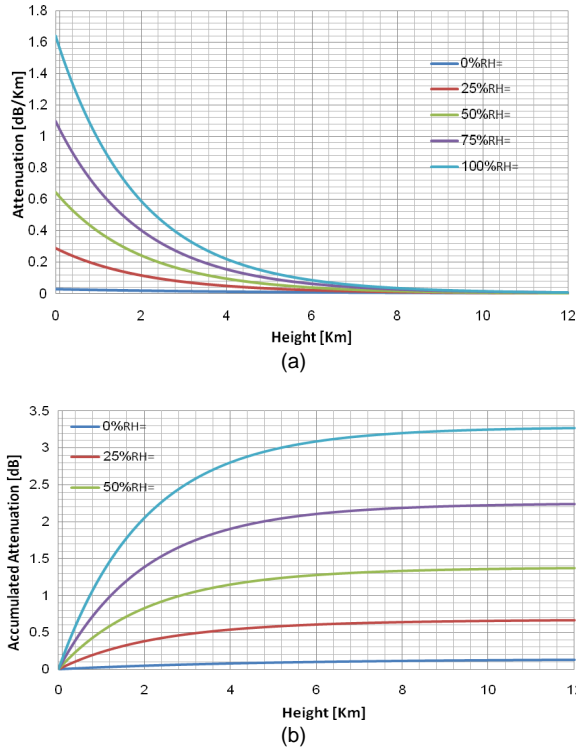


Fig. 2. Attenuation at 94GHz as a function of height above sea level: a) local attenuation coefficient $20\log(e) \cdot \alpha(f)$ in [dB/Km] and b) accumulated attenuation in [dB].

B. Evaluation of total additional attenuation

As known, free space propagation attenuation, A_{FS} , is dependant on distance and frequency:

$$A_{FS} = (4\pi d / \lambda)^2 \quad (7)$$

where d is the distance and λ is the wavelength. As example, for a GEO-Earth link in the range of 80 GHz the attenuation is of the order of 220 dB.

Free space path attenuation has to be summed (in dB) to atmospheric additional attenuation to obtain total link path loss. The additional attenuation, A_T (measured in dB), is the sum of different contributions:

- absorption of atmospheric gases (oxygen and water vapour),
- absorption, scattering and depolarization due to rain and other precipitations,
- attenuation due to clouds,
- fast fading, scintillation and others related to variations of refraction index.

Rain is the phenomenon that is responsible for the highest contribution to the total attenuation above 10 GHz (an exception occurs for frequencies near the oxygen resonance peak and low elevation angles).

In order to estimate A_T , ITU recommendations can be used [16]. These recommendations have been created

using a database of measurements performed in Q/V bands but, through frequency-scaling techniques, they can be applied to higher frequencies [17].

In Fig.3 the estimated total additional attenuation (y-axis, dB) not exceeded for a time percentage (x-axis %) is shown. The frequencies used for simulation are 86 GHz for the uplink and 76 GHz for the downlink.

The Earth station is located near Rome (Italy).

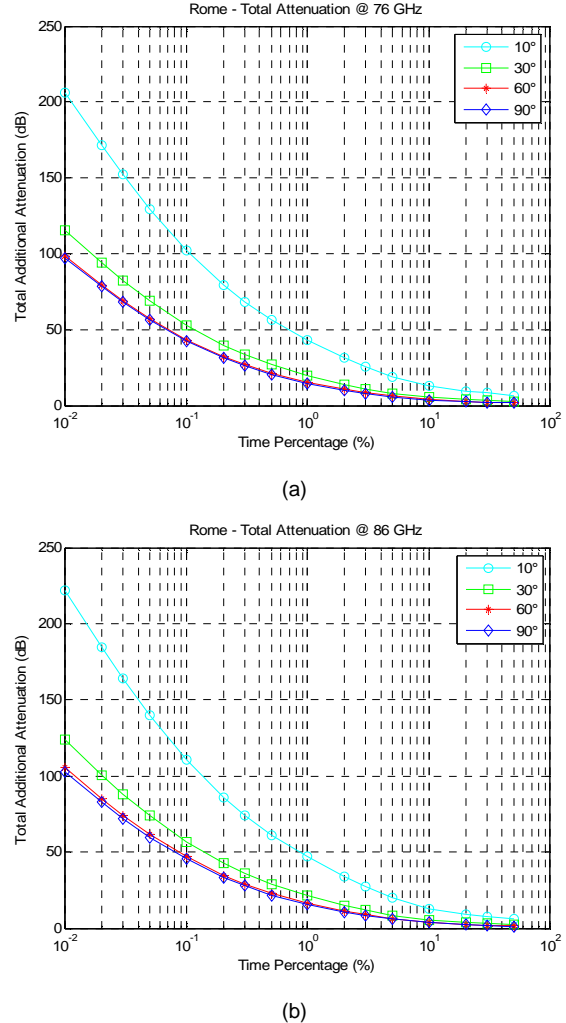


Fig.3. Total additional attenuation estimated at (a) 76 GHz and (b) 86 GHz (Rome, Italy).

3. HARDWARE IMPAIRMENTS AND LINK DISTORTIONS IN EHF SATELLITE COMMUNICATIONS

A. Satellite receiver (G/T) vs. carrier frequency

It is known that the non-ideal behavior of hardware components (working both in RF and baseband domains) has a significant impact on global

performance of satellite communication systems. Increasing the carrier frequency, these kinds of impairments may also substantially increase their impact. As mentioned in Section 2, path loss and rain fading to which an EHF signal is subjected along its propagation path may be very relevant. Therefore power resources in EHF bands are generally quite scarce and should be intensively exploited. In order to clarify such a crucial aspect, let's consider some well-known link budget expressions. The carrier-to-noise power density ratio at the input of the satellite receiver (uplink direction) is given by [18]:

$$(C/N_0)_u = (G/T)_s + (EIRP)_e - L_u - L_A + 228.6 \text{ (dB} \cdot \text{Hz)} \quad (8)$$

where: $(EIRP)_e$ is the effective isotropic radiated power by the earth-station, L_u is the free-space path loss (whose expression has been reported in Section 2) L_A is the supplementary attenuation due to atmospheric phenomena and rain (discussed in Section 2) and, finally $(G/T)_s$ is the *gain-to-noise temperature ratio* of the satellite receiver, defined as [19]:

$$(G/T)_s \triangleq 10 \log_{10} \left\{ \frac{\left(\frac{g_A^s g_{RF}^s}{L_{pol}^s L_F^s L_{pe}^s} \right)}{\left[\frac{T_A^s}{L_F^s} + T_F^s \left(1 - \frac{1}{L_F^s} \right) + T_e^s \right]} \right\} \text{ (dB/}^\circ\text{K)} \quad (9)$$

The quantities of eq. (9) can be listed as follows [19]:

- g_A^s is the satellite antenna gain;
- g_{RF}^s is the gain of the RF stage of the satellite system (amplifiers, filter, demodulator, etc.);
- L_{pol}^s is the polarization mismatch loss;
- L_F^s is the satellite feeder loss;
- L_{pe}^s is the pointing error loss due to the misalignment between transmit and receive antennas with respect to the boresight;
- T_A^s is the effective noise temperature of the satellite antenna;
- T_F^s is the equivalent noise temperature of the satellite receiver feeder;
- T_e^s is the equivalent noise temperature of the satellite demodulator.

The equivalent noise temperature, referred in (9) to payload components like antenna, feeder and demodulator, is defined as follows [19]:

$$T_{comp} \triangleq \frac{\eta_{comp}}{k} (^\circ\text{K)} \quad (10)$$

η_{comp} being the one-sided power spectral density of the thermal noise added by the payload component (with effective approximation, thermal noise is supposed additive white Gaussian noise) and k the Boltzmann's constant ($1.379 \cdot 10^{-23} \text{ W/Hz}^\circ\text{K}$).

The key point is that $(G/T)_s$ depends on the carrier frequency and, in particular, it may drop with the carrier frequency in the presence of pointing errors. In fact, considering the same antenna efficiency and the same circular antenna diameter, the antenna gain increases with carrier frequency. However, the beam pattern becomes narrower and so the antenna increases its directivity. In particular, it has been shown in [18] that the pointing error loss can be approximately expressed as:

$$L_{pe} \approx 12 \left(\frac{\theta}{\theta_0} \right)^2 \text{ (dB)} \quad (11)$$

where θ is the off-boresight angle and θ_0 is the 3dB-beamwidth angle, which is given approximately by the following equation [18]:

$$\theta_0 \approx 65 \left(\frac{c}{f_c D} \right) \text{ (degs)} \quad (12)$$

f_c being the carrier frequency, D the antenna diameter and c the speed of light. Replacing the expression of θ_0 in (11) we can obtain the final formulation of the pointing error loss as a function of the carrier frequency:

$$L_{pe} \approx 12 \left(\frac{\theta \cdot D \cdot f_c}{65c} \right)^2 \text{ (dB)} \quad (13)$$

On the other hand, the antenna gain (expressed in dB) increases with the antenna aperture and, then, with the antenna (circular) diameter as follows [18]:

$$g_A^s = 9.94 + 10 \log_{10} \eta + 20 \log_{10} (D \cdot f_c / c) \text{ (dB)} \quad (14)$$

η being the antenna efficiency ($\eta < 1$). Considering the expression of $(G/T)_s$ shown in eq. (9), it is interesting to evaluate the ratio (in dB) between the antenna gain and the pointing error loss. Numerical values of such a ratio versus carrier frequency are shown in Fig.4.

One can note that the $(G/T)_s$ drop due to pointing errors is almost irrelevant for all values of θ if the carrier frequency is less than 15 GHz (Ku-band). In the Ka-band (18-30 GHz), this drop is less than 2dB. In the W-band (75-110GHz) the related loss may become relevant even for moderate value of θ . It is worth noting that the pointing error depends on the mechanical antenna tracking system whose precision

may be impaired by strong wind and propagation fluctuations [19].

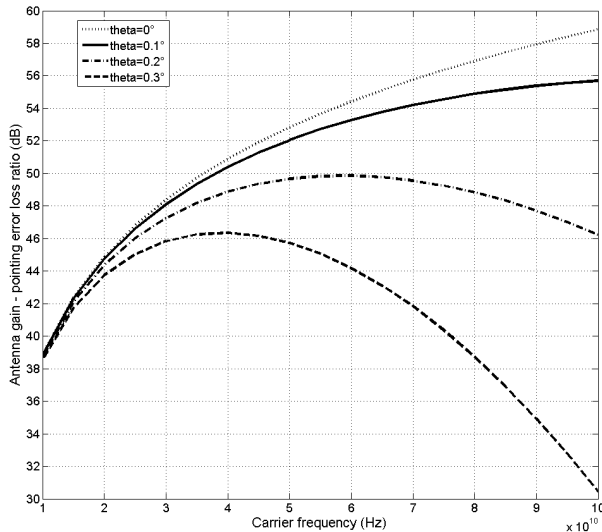


Fig. 4. Ratio between satellite antenna gain and pointing error loss (in dB) vs. carrier frequency for $\eta=0.7$, and $d=1m$.

Curves of Fig.4 clearly indicate that antenna tracking should be very precise, in particular at higher frequencies (a value for θ less or at least equal to 0.1° is strongly envisioned for EHF satellite communications). However, an additional power loss due to de-pointing of the order of 2dB should be forecast as safety margin.

B. Nonlinear distortions

In order to cope with the aforesaid link budget constraints, in EHF satellite transmissions High-Power Amplifiers (HPA) should work very close to saturation. This means that the increased power efficiency is paid for in terms of nonlinear signal distortion. Earth stations usually employ Travelling Wave Tube (TWT) amplifiers or Klystron amplifiers [18] for the uplink. On the other hand, the satellite payload generally uses TWT for high-frequency (Ku and Ka band) high-power applications (200-300 W) [18]. Solid State Power Amplifiers (SSPAs) have been used intensively for low power (10-20 W) and low frequency (less than 10 GHz) applications and for phased arrays where the power gain is distributed over a large number of elements [18]. HPAs exhibit nonlinear amplitude-to-amplitude (AM/AM) and amplitude-to-phase (AM/PM) characteristics [18]. As a consequence, the power gain of the amplifier is not constant as in linear amplifiers. An example of a power-input power-output nonlinear characteristic related to a 94 GHz Klystron designed for the earth station of the DAVID-DCE experiment [20][21] is shown in Fig. 5. This figure has been obtained from real amplifier curves reported in data-sheets from Communications and Power Industries (CPI) (Palo Alto,

CA, product series: VZB 2788). The power gain (in dB) is also plotted in Fig.5.

Nonlinear characteristics of HPAs causes unwanted effects both in the case of amplification of a single signal and in the case of multi-carrier (i.e.: FDMA) signals. They can be summarized as follows [18]:

- *Envelope distortion* on the modulated signal due to AM/AM conversion. This distortion particularly impacts system performance in the case of mixed amplitude-phase modulations (i.e.: M-QAM) and/or in the case of pulse-shaped modulations characterized by non-constant envelopes. As noted in [22], no Inter-Symbol-Interference (ISI)-free point can be observed in the eye-pattern diagram of the received Root-Raised-Cosine (RSC) signal in the presence of nonlinear distortions;
- *Non-constant phase shift* between input and output signals, as a function of the input power (AM/PM conversion). This effect is particularly harmful in the case of phase modulations (like M-PSK) or mixed amplitude-phase modulations (like M-QAM);
- *Spectral re-growth* of the RF signal that will cause adjacent channel interference and violation of spectral mask requirements, as shown in [23];
- *Intermodulation*: when several carriers are simultaneously amplified in a non-linear amplifier (FDMA case), intermodulation products are generated at spurious frequencies that are linear combinations of the modulated carrier frequencies [18]. This means that spurious replicas of modulated signals may fall inside an occupied frequency slot. The number of intermodulation products increases very quickly with the number of input carriers (for example, for 3 carriers there are 9 products and for 5 carriers there are 50).

In broadband EHF satellite scenarios, such kind of distortions may strongly decrease link performance and capacity. Modulations characterized by constant envelope, like QPSK with rectangular waveform and Minimum Shift Keying (MSK), may be more convenient for satellite communications due to less vulnerability to amplitude saturation. However, the AM/PM characteristic may produce very relevant phase jitters that can severely impair coherent demodulation.

Moreover, QPSK and MSK are both characterized by unlimited bandwidth with consequential problems of adjacent channel interference and violation of spectral mask regulations (from this viewpoint, power level of MSK secondary lobes is well below that of QPSK, even though the main lobe of MSK spans on a bandwidth which is doubled with respect to that of QPSK).

The typical solution adopted in PHY-layer satellite design is based on backing the transmitted power in order to avoid non-linear effects [18]. As mentioned, such a solution is not welcome in EHF broadband scenarios. The Klystron amplifier, whose nonlinear

characteristic is drawn in Fig.5, requires an input back-off¹ (IBO) equal to 4dB, corresponding to an output back-off (OBO) of 2dB, in order to work in the linear zone. Some examples presented in the literature related to prototypes of HPAs working in the EHF domain [24-27] exhibit similar values of IBO and OBO, as shown in Tab.1. OBO may have a serious impact in the EHF link performance, as clearly shown in [28]. In fact, the signal power reduction due to OBO involves an additional loss to be added to other losses of an already constrained link budget. It is clear that a further power sacrifice, although necessary to guarantee acceptable link performance, substantially decreases link capacity, in particular when high-data rate applications are considered.

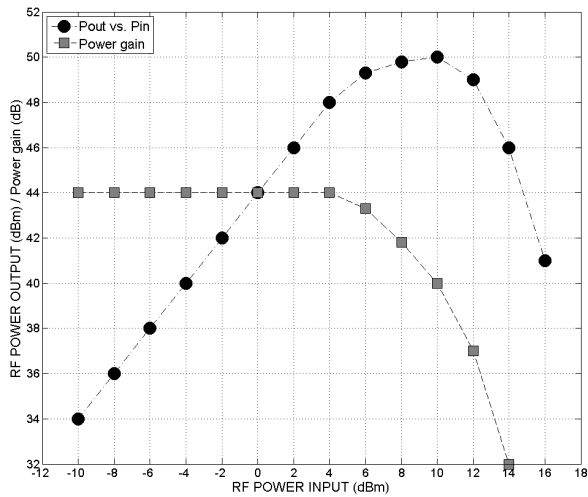


Fig. 5. Example of nonlinear transfer power characteristic of a 94 GHz Klystron amplifier for satellite applications (thanks to CPI).

Tab. 1. Examples of Input Back-off (IBO) and Output Back-Off (OBO) values of state-of-the-art EHF HPAs.

REF, TYPOLOGY, APPLICATION	FREQUENCY	IBO (dB)	OBO (dB)
[24] Gyro-klystron, radar	94 GHz	5.0 dB	3.0 dB
[25] TWT, airborne app.	90.6 GHz	5.0 dB	4.0 dB
[26] CMOS, radar	75-95 GHz	10.0 dB (@ 77 GHz)	2.5 dB (@ 77 GHz)
[27] Helix TWT, satellite	44 GHz	6.0dB	2.0 dB

An alternative solution to power back-off is represented by amplifier linearization. Conventional pre-distortion linearizers are very effective to reduce

nonlinear distortion effects if the TWT is operated well below saturation [29]. The drawback of a canonical pre-distortion linearizer, based on the pure compensation of the nonlinearity, is that it exhibits rapid amplitude depression and large phase shift at or beyond saturation [18]. In order to allow the use of TWT very close to saturation more sophisticated linearizers have been proposed in the literature. An example of these is reported in [29], where a soft-limiter type linearizer has been implemented by employing a standard pre-distortion linearizer followed in cascade by an amplitude limiter. A very recent work dealing with wideband linearization of TWTAs has been proposed by Katz, Gray, and Dorval in [30]. The choice about analog and digital linearization has been discussed in [30] in the wideband case. For wideband applications, digital linearization based on DSP is not advisable due to cost, power consumption and limited hardware processing capabilities (multigigahertz DSP are not available). Because of these limitations, analog linearizer solutions are preferred. One of the challenging aspects of practical TWT linearization is the necessity of changing linearizer's gain and phase transfer characteristics over frequency, as the gain and the phase of the amplifier at different frequency may change. Such an operation may be not trivial when very high frequency broadband signals are transmitted. The resulting gain ripple can be a serious problem, as it may degrade the amplifier linearization and reintroduce inter-modulation.

To conclude this sub-section, we can say that nonlinear distortion in W-band broadband satellite links should be compensated and/or counteracted rather than avoided by means of power back-off. The objective to be achieved is to maintain the amplifier gain as much higher as possible with negligible distortion and without decreasing spectral efficiency. This last is still a tradeoff. Practical PHY-layer solutions to this problem, based on properly-designed pulse-shaped modulations and distortion compensation, will be discussed in Section 4B.

C. Phase-noise

Phase-noise is an unwanted phase modulation of a signal and can be viewed as spurious sidebands on a wanted carrier. An ideal local oscillator is a fixed single-frequency source, but in reality there are always some rapid fluctuations around the nominal frequency. This fluctuation will be passed, via the frequency conversion process, into the signal path. The equation of a carrier affected by phase-noise is given as follows:

$$x_c(t) = A_c \cos(\omega_c t + \phi_n(t)) \quad (15)$$

The phase-noise is the random process $\phi_n(t)$. It is clear from equation (15) that phase-noise is not an additive

¹ The input back-off is defined as the ratio between the input average power at saturation and the actual operating input average power. The definition of the output back-off is the analogous (replacing input by output) [18].

noise. Therefore, its impact on link performance should be adequately evaluated.

Higher-frequency oscillators generally have higher phase-noise associated with them, but nonlinear amplifiers may also increase the phase-noise of a processed signal. In Fig.6, a noisy oscillator output measured by a spectrum analyzer is shown. One can note that the main frequency row, corresponding to the oscillator fundamental frequency, presents a kind of “skirt” that actually indicates the “impure” carrier tone (the other row is a spurious harmonic).

It is clear from Fig.6 that phase-noise should be conveniently evaluated in the frequency domain versus the frequency offset with respect to the fundamental carrier frequency f_c , rather than versus the absolute frequency. Let's denote such an offset with Δf .

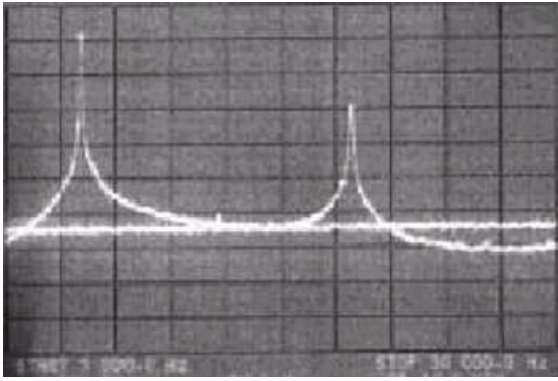


Fig. 6. Noisy oscillator output measured by a spectrum analyzer.

Starting from these considerations, a possible modeling of phase-noise, commonly employed in practical applications, has been proposed in [31]. Such a model is based on two assumptions: i) the phase noise is assumed to be asymptotically stationary, and ii) the oscillator input perturbation is assumed to be white Gaussian-distributed thermal noise. Under these assumptions, the analysis shown in [31] pointed out that the single-sideband (SSB) phase-noise power spectral density (PSD) of an ideal oscillator (made of a lossy RLC resonator and an ideal energy restoring circuit) is proportional to $1/(\Delta f)^2$, i.e.:

$$S_{\phi}(\Delta f) = 2kT \left(\frac{f_c}{2Q\Delta f} \right)^2 \quad (\text{W} \cdot \text{rad}^2/\text{Hz}) \quad (16)$$

T being the noise figure and the equivalent noise temperature of the oscillator, k Boltzmann's constant and Q the so-called *unloaded tank* of the oscillator defined in [31] as:

$$Q = \frac{1}{2\pi GLf_c} \quad (\text{rad}^{-1}) \quad (17)$$

where G and L are the conductance and the inductance of the oscillator circuit, respectively. It is traditional to normalize the SSB power spectral density of phase-noise to the average carrier power and to express this ratio in logarithmic scale. Performing this normalization, we obtain the following equation for the normalized SSB power spectral density:

$$\Lambda_{\phi}(\Delta f) = 10 \log \left[\frac{2kT}{P_c} \left(\frac{f_c}{2Q\Delta f} \right)^2 \right] \quad (\text{dB} \cdot \text{rad}^2/\text{Hz}) \quad (18)$$

As a consequence, the typical phase-noise specification defines the maximum sideband levels, relative to the carrier, at a certain frequency offset Δf from the carrier frequency f_c [31]. These units are thus proportional to the log of a power spectral density normalized with respect to the carrier power. Therefore, the usual measure of phase noise PSD is given in terms of *decibels below the carrier (dBc)* over Hz for a given frequency offset Δf to the fundamental frequency.

A drawback involved by the use of such a model is that low-frequency noise spectral components proportional to $1/f$ (like, e.g., flicker noise) are completely ignored. A more realistic and comprehensive model of phase-noise (*Leeson model*) is given as [31]:

$$\Lambda_{\phi}^L(\Delta f) = 10 \log \left[\frac{2FkT}{P_c} \left\{ 1 + \left(\frac{f_c}{2Q\Delta f} \right)^2 \right\} \left(1 + \frac{\Delta f_{1/f^3}}{|\Delta f|} \right) \right] \quad (19)$$

The modifications with respect to the conventional model consists of a factor F to account the increase of noise in $1/(\Delta f)^2$ region, an additive factor of unity (inside the braces) to account for noise floor and a multiplicative term (that one in the second set of parentheses) to account a $1/(\Delta f)^3$ behavior for small offset frequencies. $\Delta f_{1/f^3}$ is a parameter taking into account the presence of non-white noise components affecting the oscillators. Apparently, the increase of the carrier power and the increase of Q (keeping constant the other parameters) may reduce the phase noise. Increasing signal power improves the ratio as the thermal noise is fixed. The increase of Q quadratically improves the ratio, as the tank impedance of the RLC resonator falls off with $1/Q\Delta f$. These heuristic assumptions are reasonable and make sense in many practical situations. However, it is observed in [31] that

an increase of Q is accompanied by an increase of F . Therefore, a bit of attention should be paid in considering the validity of such assumptions. A revision of phase noise theory is presented in [31], which is obtained by relaxing the hypothesis of system linearity and stationarity of phase noise. Such revision work lead to the conclusion that a good oscillator should anyway maximize carrier power and resonator Q , keeping constant all other factors. In addition, it is noted that an active device is always necessary to compensate for tank loss, and that active devices always contribute to noise.

In order to guarantee frequency stability and low-phase-noise, the choice of Gunn diode oscillators has been used for almost 25 years as a valuable and cost-effective solution to implement frequency sources in the EHF domain. Practical examples are shown in the literature related to 35 GHz oscillators [32], 90 GHz oscillators [33] and W-band phase locked loops [34-35]. The phase-noise level reached by these devices is generally less than -100dBc/Hz at a frequency offset of 100 KHz. An actual phase-noise mask for a 91.25 GHz oscillator is shown in Fig.7 obtained from data provided by Orelikon Contraves Italiana S.p.A. (now Rheinmetall Italia S.p.A.). Such a component has been studied in the framework of the DAVID-DCE experiment and proposed as local oscillator for the earth station. The circuit is based on a Gunn oscillator (running at about 90 GHz) to lock a 15 GHz frequency generated by a Phase Locked Dielectric Oscillator (PLDRO) driven by a quartz oscillator. The oscillator of Fig.7 exhibits a phase-noise level equal to -95dBc/Hz at a frequency offset of 100 KHz that is in line with that one of low-noise Gunn oscillators.

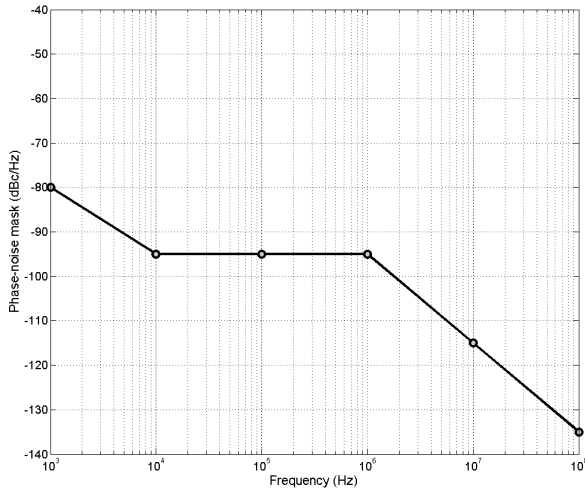


Fig. 7. Phase-noise mask of a 91.25 Ghz oscillator (thanks to Orelikon Contraves italiana S.p.A, now Rehinmetall Italia S.p.A).

The effect of phase-noise in coherent demodulation is to produce a residual phase jitter (hereinafter denoted

by ψ) at the output of a generic phased-locked loop (PLL). Under the hypotheses previously assumed for phase-noise, ψ is a Gaussian random variable with zero mean and standard deviation that can be expressed as follows [36]:

$$\sigma_{\psi} = \sqrt{2 \int_{B_L}^{R_s/2} \lambda_{\phi}(\Delta f) d\Delta f} \quad (\text{rad}) \quad (20)$$

where B_L is the carrier recovery loop bandwidth, R_s is the symbol rate, and $\lambda_{\phi}(\Delta f)$ is the one-sided normalized phase-noise PSD of (18) and/or (19), converted from dBc/Hz to rad^2/Hz . It should be noted that the total residual phase jitter affecting a coherent demodulation is given by the sum of ψ with the residual phase jitter due to thermal noise. The total residual phase jitter, hereinafter denoted with Φ , is a Gaussian random variable with zero mean and standard deviation given as follows [36]:

$$\sigma_{\Phi} = \sqrt{\sigma_{\psi}^2 + \left(\frac{N_0 B_L}{2E_s R_s}\right)^2} \quad (\text{rad}) \quad (21)$$

N_0 is the power spectral density of the AWGN and E_s is the energy transmitted per symbol.

As far as the digital demodulation task is concerned, this residual phase jitter may critically impact on symbol decision and, therefore, on system performance in terms of bit-error-rate. In [36], closed form expressions for the Bit Error Probability (BEP) of a BPSK and QPSK modulation affected by random phase jitter are provided. We show these expressions in equations (22) and (23).

$$P_b = \frac{1}{2} \int_{\Phi} \text{erfc} \left(\sqrt{\frac{E_b}{N_0}} \cos(\phi) \right) p_{\Phi}(\phi) d\phi \quad (\text{BPSK}) \quad (22)$$

$$P_b = \frac{1}{4} \int_{\Phi} \text{erfc} \left(\sqrt{\frac{E_b}{N_0}} \cdot (\cos(\phi) - \sin(\phi)) \right) p_{\Phi}(\phi) d\phi + \frac{1}{4} \int_{\Phi} \text{erfc} \left(\sqrt{\frac{E_b}{N_0}} \cdot (\cos(\phi) + \sin(\phi)) \right) p_{\Phi}(\phi) d\phi \quad (\text{QPSK}) \quad (23)$$

$p_{\Phi}(\phi)$ is the Gaussian probability density function of the total residual phase jitter. On the basis of these expressions, the BER degradation for different values of σ_{Φ} has been computed. Results are shown in Fig.8 and Fig.9 for BPSK and QPSK modulation respectively.

From Fig. 8 and 9, we can note that for $\sigma_\phi = 7^\circ$, the BER degradation with respect to the ideal AWGN curve at $E_b/N_0=10\text{dB}$ equals to less than 0.1dB for BPSK modulation and 1.5dB for QPSK modulation.

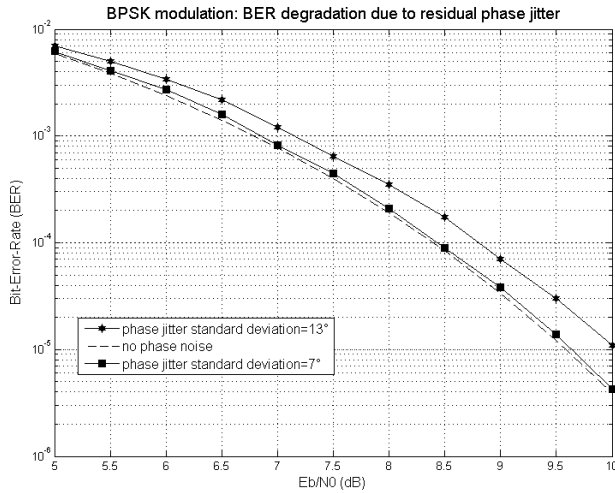


Fig. 8. BER degradation vs. E_b/N_0 with respect to different values of residual phase-jitter standard deviation (BPSK modulation)

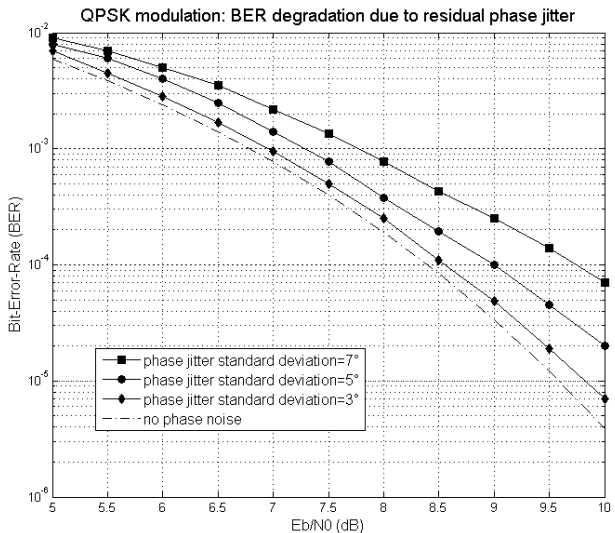


Fig. 9. BER degradation vs. E_b/N_0 with respect to different values of residual phase-jitter standard deviation (QPSK modulation)

In Fig.8, we do not show results for $\sigma_\phi < 7^\circ$, as the achieved BER degradation is irrelevant. We added a curve achieved for $\sigma_\phi = 13^\circ$ just to show how different modulation formats behave with larger phase jitters (the degradation with respect to the ideal BER curve of BPSK is about 0.4dB). Results shown in Fig.8 and Fig.9 seem to demonstrate that the adoption of spectrally-efficient multi-level modulations (like M-ary PSK or M-ary QAM) using coherent demodulation may be not advisable in the presence of relevant phase-noise levels.

In non-coherent systems, the relationship between phase-noise spectrum and system degradation is not so evident, since no phase error is actually generated [37]. Instead, non-coherent energy detection is generally employed for data decoding, and any short-term phase noise appearing on the modulated carrier must be converted in effective energy changes in order to evaluate data decisioning [37]. The authors of [37] proposed a formal evaluation of oscillator phase-noise for non-coherent data detection of DPSK and FSK modulated signals based on a truncated Taylor series expansion of the bit-error-probability where the phase noise spectrum directly appears. Crystal and Cesium oscillators have been considered in [37] and simulation results reported that the phase-noise does not significantly degrade system performance when the carrier frequency is less than 10 GHz. To summarize the contents of this paragraph, we can say that phase-noise may be a critical impairment factor to be carefully appraised in W-band PHY-layer design. Phase-noise typically drives the choice of the modulation format that should guarantee robustness against frequency instability and residual jitters, minimizing the BER degradation. In Section 4.A, some feasible phase-noise driven PHY-layer solutions will be proposed and discussed.

4. RADIO INTERFACES (PHYSICAL LAYER SOLUTIONS)

The design choices of the RF and baseband part of a broadband EHF satellite needs to consider the following factors:

- High level of phase noise
- Non-linearities mainly due to the HPA
- Propagation impairments (especially related to tropospheric precipitations)

Each of the previous factors calls for specific design choices that must be driven also by the following requirements: high spectral and power efficiency, low complexity, small mass and volume of the payloads.

A. Phase noise-driven design

As outlined in the previous section, the generation of EHF frequency bands, assuming a typical heterodyne receiver, gives rise to high levels of phase noise. In order to reduce performance degradation, the following *not-alternative* solutions can be considered:

- 1) Reduction of the phase noise level by properly designing the RF part [38];
- 2) Design of IF and baseband parts (modulation, channel coding, carrier recovery) that are robust to phase noise.

Lower phase noise levels, as well as reduced mass, volume and complexity are the main reasons that lead to the use of direct conversion receivers already at Ka-band [39]. Direct conversion allows a reduction of the circuit complexity due to the elimination of intermediate conversion stages and corresponding LO sources. On the other hand, one of the most critical parameters in such circuits, especially at high frequency, is the imbalance between I and Q components that will result in signal degradation in the form of distortion or offset in the signal constellation. Self-calibration techniques have been proposed to mitigate the imbalance [40].

Regarding the baseband part, high levels of phase noise limit the use of high order modulations and hence, the achievable spectral efficiency. A state of the art modulation solution (known since mid of 60's), which provides easy carrier recovery and robustness against phase-noise effects, has been proposed in [21] for the DAVID-DCE PHY-layer design. Such a solution is based on a Split-Phase Manchester-coded BPSK (SP-BPSK) constellation with modulation index equal to 60° . Such a technique provides a residual carrier in the spectrum. If the channel bit-rate significantly exceeds the Doppler frequency, the residual carrier can be extracted and used to pilot a simple 2nd order Phase-Locked-Loop (PLL) circuit. The SP-BPSK solution provides very effective carrier recovery in terms of reduced convergence time and reduced phase jitter even in the presence of large uncompensated Doppler shifts. The price to be paid is in terms of reduced spectral efficiency (equal to 0.5b/s/Hz) and reduced power efficiency (the power loss due to the residual carrier is 3dB with respect to conventional BPSK).

The use of spectrally efficient modulations in an EHF context would require the combined use of efficient carrier recovery and robust channel coding. In [41], a robust approach for carrier recovery of M-QAM modulations has been proposed for broadband W-band LEO satellite connections characterized by the presence of phase-noise and high Doppler shifts. The carrier recovery loop of [41] effectively counteracts slow convergence and frequency mistracking characterizing state-of-the-art circuits. However, the residual phase jitter is imposed by the phase-noise PSD, as clearly shown in eq. (20). The adoption of efficient channel coding may represent a solution to this problem. A good tradeoff between spectral efficiency and robustness may be offered by Trellis-Coded-Modulation (TCM) [42]. The study of TCM in a W-band LEO scenario has been presented in [43]. The vulnerability of coherent TCM with respect to phase jitters together with the necessity of power back-off to avoid nonlinear distortions seems to privilege the use of robust TCM configurations like, e.g.: Ungerboeck's 2/3 trellis coding with 8-QAM and 3/4 trellis coding with 16-QAM. Other

TCM configurations, characterized by increased spectral efficiency (like 5/6 trellis coding with 64-QAM) can be adopted only when phase-noise is almost null. This trend is clearly shown in Fig. 10, which reports some simulation results related to the W-band LEO scenario of [43] considering: a) data-rate of 1 Gb/s, b) presence of nonlinear distortions, c) carrier recovery performed by the loop proposed in [41]. The residual phase jitter for the TCM configurations considered in [43] decreases, as expected, with the baud-rate (see Tab.2). However, the impact of phase jitter on BER performance is more relevant as the number of levels of the constellation increases. A possible alternative solution may consider the adoption of turbo coding and turbo trellis-coded modulations to EHF satellite scenarios. Some works presented in the literature considered the use of turbo-coding and turbo-TCM to mobile satellite channels. In [44], El-Awadi et. al. assessed concatenated turbo-TCM in mobile satellite transmissions. Results shown in [44] evidence that turbo-TCM may improve system robustness both in presence of Rayleigh fading and non-linear distortion. Turbo coding is also considered in [45] for shared satellite channels with collisions. In this framework, it is worth mentioning the work of Howard and Schlegel [46], where a novel approach for turbo-coded differential modulation. It is known that differential modulation is insensitive with respect to phase jitters, as it evaluates the difference between two received samples in order to decide the transmitted symbol. The robustness of the proposed coded-modulation scheme is appreciated also in the presence of relevant phase jitters thanks to a simple channel estimation scheme that can avoid the necessity of channel state information knowledge. This makes differential turbo-coded modulation a valuable candidate for future applications in EHF satellite scenarios where phase noise represents a serious issue.

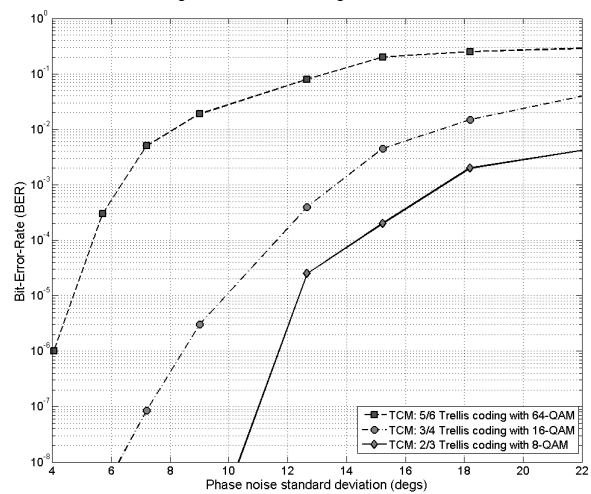


Fig. 10. BER at the output of the TCM decoder for a 1 gbit/sec. W-band LEO satellite connection.

Tab. 2. Residual phase jitters for TCM schemes of Fig.10.

$S_o(f)_{f=10kHz}$	$\sigma_o(8-QAM)$ ($R_s = 500$ Mbaud/s)	$\sigma_o(16-QAM)$ ($R_s = 333$ Mbaud/s)	$\sigma_o(64-QAM)$ ($R_s = 200$ Mbaud/s)
-70dBc/Hz	19.85°	16.21°	12.81
-75dBc/Hz	11.16°	9.11°	7.21
-80dBc/Hz	6.27°	5.12°	4.05
-85dBc/Hz	3.52°	2.88°	2.27

B. Non-linear distortions-driven design

Impairments due to non-linear distortions can be mitigated through two basic baseband design choices:

- 1) Proper design of the modulation to be used.
- 2) Use of pre-distortions techniques

Traditional QAM (Quadrature Amplitude Modulation) constellations and pulse-shaped modulations like RSC-QAM have a high peak-to average power ratio (PAPR) that cause non-negligible AM/AM and AM/PM distortions when the signal is amplified by an HPA that works in the non-linear part of the characteristic. In this context, constant envelope modulations are preferable. GMSK is a constant-envelope modulation scheme with fast roll-off property, and hence, it is a good choice for maximally using the HPA (assuming single carrier) [47]. However, its theoretical bandwidth efficiency is only around 1.33 bits/s/Hz. In order to keep the modulated signal envelope as compact as possible, without sacrificing spectral efficiency, the use of non-conventional pulse shaping may be considered. In this context, a very innovative solution has been proposed in [28] based on the Prolate Spheroidal Wave Functions (PSWFs). PSWFs were firstly studied by D. Slepian and H. Pollack (Bell Labs) in 1961. The fundamental concept standing at the basis of PSWF is to concentrate the energy of the pulse in limited regions, both in time and frequency domains. PSWFs are characterized by some interesting properties; the most important one is that PSWFs exhibit by definition an optimized tradeoff between concentration of the energy in a finite time window and in a finite bandwidth: this means that the resulting modulated signal is characterized by “almost finite” pulse duration and, at the same time, “almost limited” bandwidth. In addition, PSWFs of order 1 and order 2 are characterized by envelope compactness that is clearly demonstrated by Fig. 11, depicting the order 1 PSWF (the order 2 PSWF is very similar and, then, it has been omitted). Such observation inspired the authors of [28] to use order 1 and order 2 PSWFs as in-phase and quadrature components of a 4-level modulation, i.e.: the 4-ary Pulse Shape Modulation (PSM) scheme proposed in [48]. As the Peak-to-Average Power Ratio of the 4-ary PSM modulation is only 1dB (instead of 3.22dB, measured for RSC-filtered QAM [28]), power amplification can be done in saturation without losing power efficiency and introducing appreciable waveform distortion. The thorough analysis of [28] pointed out that PSWF-based 4-ary PSM performs slightly better

than GMSK in terms of BER. The substantial improvement with respect to RSC-filtered QAM and GMSK is achieved by PSWF waveforms in terms of increase of normalized spectral efficiency that is measured in percentages of 25%-36% depending on application scenarios (normalized efficiency is defined in [28] as the ratio between the achievable net payload rate and the bandwidth occupied by the RF signal). Another interesting solution, which has been adopted by the DVB-S2 standard, is the use of multi-level Amplitude- and Phase-Shift Keying (APSK) constellations based on concentric “rings” of equispaced points [49],[50]. In APSK, the modulation symbols bear two different amplitudes only, thus minimising envelope fluctuations in the transmitted signal. This results in lower distortions onto the HPA-amplified received signal. By proper Minimum Euclidean distance-based APSK constellation parameter optimisation, APSK showed superior performance over non-linear satellite channels and almost identical performance compared to QAM over linear AWGN channel [49].

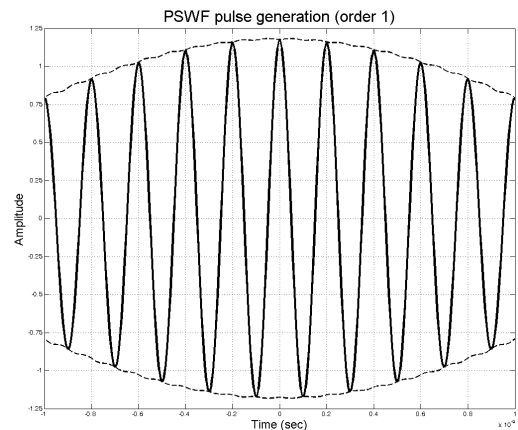


Fig.11. Prolate Spheroidal Wave Function (PSWF) of order 1.

The second approach to minimise the effect of non-linearity is adaptive constellation (data) pre-distortion in the transmitter. Pre-distortion means intentionally modifying the location of the data symbols on the complex plane with respect to their nominal position. Such a technique only calls for a modification of the transmitted constellation points, without the need to resort to analog devices. This is particularly straightforward and effective for circular constellations such as APSK. Details are discussed in [51]. Different pre-distortion schemes have been investigated, based either on “instantaneous” evaluation of the distortion at the receiver (adaptive *static* pre-distortion), or with the consideration of a certain amount of “memory” in the combined phenomenon of non-linear distortion plus matched filtering at the

receiver (so called adaptive *dynamic* predistortion) [52]. In [53], it has been shown that with pre-distortion, the HPA can be operated remarkably close to saturation, e.g. down to 1.5 dB average Output Back-Off in the case of 16-point constellations with highly-efficient channel coding (Turbo or Low-Density Parity Check (LDPC) codes).

C. Propagation Impairments Mitigation Techniques

Some important limitations of EHF satellite communications arise from the high propagation impairments. In this framework, techniques able to improve system availability and throughput have to be developed.

In order to counteract atmospheric attenuation high system static link margins could be used to minimize outage duration of the services. Fixing high static link margins is in contrast with technology limitations, both on space and ground segments, and with system efficiency. In this context PIMT (Propagation Impairments Mitigation Techniques, also known as Fade Mitigation Techniques) have to be used; these techniques aim to compensate for fades optimizing the use of system resources [54]. PIMT allow systems with rather small static margin to be designed, while overcoming (both in real-time or in post-processing) cloud attenuation, a fraction of rain attenuation, scintillation, and depolarisation events. Three main categories of PIMT can be identified:

- Diversity Techniques,
- Adaptive Techniques,
- Layer 2 techniques.

The first ones include spatial, time and frequency diversity; these techniques try to solve the problem of fades by moving around them. This can be done:

- in space, sending the information on a different route to the one that is suffering a high fade (changing the satellite or the ground station);
- in the time or frequency domains, transmitting at a different time or in a different frequency band, respectively.

These techniques are optimized to make the probabilities of each signal being affected by a fade statistically uncorrelated. For EHF satellite communications frequency diversity is not useful to cope with high atmospheric attenuation (high rain fades); as a matter of fact, in the EHF band changing the frequency does not significantly reduce atmospheric additional attenuation (notably in the upper part of the spectrum). Even satellite diversity is not a good choice if the Earth terminal is subject to a high rain fade, in fact changing the satellite does not create a signal path that is not subject to different weather conditions.

The diversity techniques that could be used in EHF satellite communications are site diversity and time diversity; these two techniques are able to create signal paths that are statistically uncorrelated with respect to the atmospheric fades

Adaptive techniques change some aspect of the system set-up to compensate for fades. For instance, in adaptive up-link power control, the ground transmit power is increased to compensate for the effects of a fade. Another adaptive technique is called ACM (Adaptive Coding and Modulation); it aims at compensating fading by changing coding or modulation scheme with respect to the propagation channel conditions. Adaptive techniques allow transmission characteristics to be adapted to the propagation channel conditions and to the service requirements for the given link. As an example, in [55] the authors optimized an ACM technique for satellite links operating in the W-band (with reference to DVB-S2 standard) providing updated thresholds for mode/code change.

Layer 2 techniques do not properly mitigate the fade event but rely on the re-transmission of the data. These techniques are based on concepts like Automatic Repeat Request (ARQ) and Time Diversity (TD) that are not best-suited for real-time applications.

D. New Research Directions

D.1. Impulse Radio or Continuous wave?

In order to answer to the need for a communication system that is robust to the non-idealities presented in Section 3 and also able to deliver very high data rates (of the order of multi-gigabit/s), a joint design of the RF and baseband parts could represent a non avoidable path to follow.

Moving in this direction, we wonder if impulse-radio communications, such as IR-UWB (Impulse-Radio Ultra WideBand) could represent a suitable choice for the physical layer. UWB has well known advantages in some terrestrial applications. IR-UWB in use for terrestrial applications and working at around 1GHz center frequency does not require the up-conversion section, whose design is usually critical at EHF bands as it includes mixers and oscillators that cause phase-noise and nonlinearities. However, this advantage does no longer hold when the center frequency is moved at frequency bands above 60GHz. In this case, we need to talk about pass-band UWB and an up-conversion section is needed. However, in [56] the authors have implemented a way to generate impulses at W-band minimizing the need for mixers and oscillators. The idea is to generate pulses with bandwidths in the order of hundreds of Gigahertz followed by a bandpass filtering stage which "locate" the signal spectrum around the desired center frequency. This architecture is pretty challenging. First of all, it needs strict control on the

ultra-short pulse generator in order to “center” the maximum of the pulse spectrum in the desired W-band frequencies. Moreover, it needs high transmitter front-end amplification, as the longest part of the power is lost by filtering.

However, even assuming a classical direct conversion transceiver, some recent work has shown that impulse-radio based communications are more robust to the channel impairments than continuous wave ones operating beyond 60 GHz [57]. In [57], the authors carefully model all the non idealities of the RF components for a W band satellite P/L and then compare the BER of a PPM (Pulse-Position Modulation) TH (Time-Hopping) IR UWB architecture and of a single carrier FSK scheme (with the same data rate and bandwidth occupation). As shown in Fig. 12, while under ideal conditions, the 2-FSK scheme outperforms the IR-UWB, when all non-idealities are considered, the BER of the IR-UWB scheme is slightly better than that of the 2-FSK.

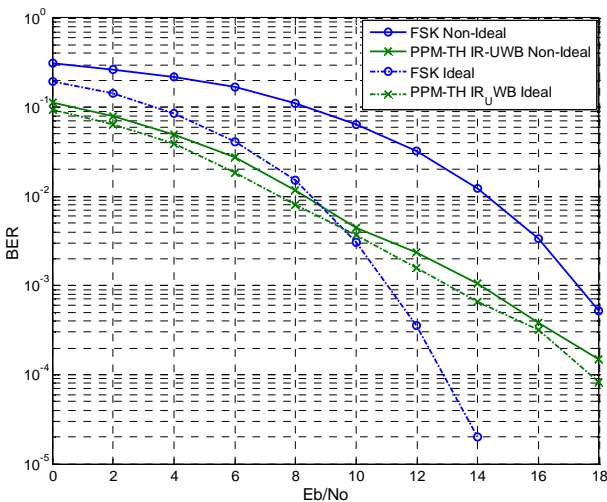


Fig. 12. PPM-TH IR-UWB vs. single carrier FSK BER performance analysis, considering RF non idealities.

D.2. Single-carrier or Multicarrier?

The employment of multicarrier techniques like Orthogonal Frequency Division Multiplexing (OFDM) and Single Carrier Frequency Division Multiple Access (SC-FDMA) in satellite environment has been discussed in the literature [58][59]. In these works, the competition single-carrier vs. multicarrier does not yield a clear winner. The main theoretical advantage of multicarrier methodologies lies in the increased flexibility and efficiency in spectrum resource management. Adopting an OFDM-based air interface, also for the satellite part of a hybrid satellite-terrestrial system, could reduce terminal complexity. This is the reason that has led to the adoption of OFDM for DVB-SH, with proper modifications and enhancements with respect to the DVB-H OFDM air interface. On the other

hand, an OFDM signal is characterized by high amplitude fluctuations that produce large Peak-to-Average-Power-Ratio (PAPRs). This makes OFDM very sensitive to non-linear distortions. PAPR reduction techniques have been extensively studied and can be applied to satellite communications. Recently it has been proved that the adoption of strong channel coding techniques in conjunction with the use of non linear distortion compensation techniques can lead to satisfactory performance even when operating close to amplifier saturation [60], [61]. A breakthrough in the utilization of OFDM in satellite communications is represented by the novel concept of Constant Envelope OFDM (CE-OFDM) [62]. CE-OFDM transforms the OFDM signal, by way of phase modulation, to a signal designed for efficient power amplification. At the receiver, the inverse transformation — phase demodulation — is applied prior to the conventional OFDM demodulator. The phase modulation transform results in constant envelope signals. CE-OFDM is shown to compare favorably with conventional OFDM in multipath fading channels when the impact of nonlinear power amplification is taken into account.

On the other hand, being substantially a single-carrier modulation, SC-FDM is characterized by much smaller PAPR than OFDM. Therefore, SC-FDMA may be considered as a valuable solution for future applications in EHF satellite communications. Potential advantages that could be taken by the use of SC-FDMA are also related to its capability to establish orthogonal frequency channels for each user’s signal, so this scheme can achieve FDM without guard bands.

In [63], an analysis of nonlinear distortion in SC-FDMA systems is assessed. Two usual SC-FDMA schemes are considered: Interleaved-FDMA (IFDMA) where users are spread over a wide bandwidth by means of interleaving and Localized-FDMA (LFDMA) where frequency components of each user cover contiguous blocks. Outcomes of [63] show that IFDMA exhibits better performances than LFDMA in the presence of saturating HPAs both in terms of reduced BER and of reduced out-of-band emissions. The large bandwidth availability typical of EHF domain should increase IFDMA efficiency even in the presence of nonlinear distortion and phase-noise.

5. NETWORKING AND APPLICATIONS

EHF frequency bands, such as the Ka-Band (20-30 GHz), Q-V band (40-50 GHz) and W band (76-110 GHz) offer the bandwidth to support future broadband satellite networking. High capacity EHF satellite communication systems may someday support data rates from 100s of Mbps to Gbps; similar to short range terrestrial wireless systems. The potential for high-date

rate communication coupled with wide area coverage makes satellite communication a good choice for future high-speed Internet access especially to locations where the terrestrial infrastructure is limited, lacking or damaged. Various EHF satellite systems were proposed in the 1990s for providing such services. Most of these failed to catch on at the time. More and more though, it seems that their time has come. In this section, we review EHF systems and services that have been proposed, consider future systems and services, examine key issues for broadband EHF satellite networks and discuss the potential impact of emerging technologies.

A. Broadband EHF systems and services

A summary of broadband EHF satellite systems is provided by Table 3 [64-73]. Some have been implemented others have not. Collectively, they illustrate a progression towards high data rate, EHF, two-way, Internet access.

Broadband EHF satellite systems may consist of one or many satellites. In the limit, the satellite network becomes an extension of high-speed terrestrial networks. In which case, on-board routing (OBR) and on-board switching (OBS) become increasingly important. This is perhaps especially the case with LEO satellite systems. An example is provided the Teledesic system proposed in the 1990s. The constellation consisted of 288 satellites in 12 planes of 24 satellites. Teledesic was to be a Ka-Band system with 60 GHz cross-links between adjacent satellites in each orbital plane. It was designed as an "Internet-in-the-sky" offering high quality voice, data and multimedia information services with fiber-like QoS performance ($BER < 10^{-10}$) to users worldwide. The planned network capacity was 10 Gbit/s with user connections of 2 Mbit/s on the uplink and 64 Mbit/s on the downlink. Although complex, costly and ultimately cancelled, it remains a prime example of a broadband satellite Internet system.

Today, almost a decade later, the trend in broadband EHF is typified by systems such as Hylas, Spaceway, Telesat, Tooway, WildBlue and O3b (see also section 6, experimental Q/V band systems). All of these systems support broadband communication for applications and services such as high-speed, two-way Internet access (e.g. video download, data download and upload), Direct Video Broadcast to homes (e.g. IPTV) and business services (e.g. VSAT, corporate networking), but they are much simpler than their predecessors Teledesic and SkyBridge. Hylas, Telesat, Tooway and WildBlue consist of a few geostationary satellites with Ka-band transponders providing regional coverage. Spaceway and O3b are exceptions with MEO satellites supporting low latency services (e.g. VoIP).

High-speed Internet access, combined with low BER and low latency, offers the potential for cable replacement. In this regard, though fiber rates may be much higher than satellite, constraints on the rates to homes [74] may limit access (e.g. 50 Mbps) making satellite not only competitive but potentially even superior. Where delay is low (e.g. LEO or MEO-based systems such as O3b), VoIP and other low-latency services can be supported. Broadband EHF is also well suited to support VSAT networks. The impact on link availability and margin due to rain and atmospheric effects, even at higher bands (e.g. V-band), is less significant for store-and-forward type VSAT type applications.

B. Trends and issues for broadband satellite networks

As can be seen from Table 3, over the past decade, the trend has been towards simpler systems with fewer satellites, and ultimately lower cost. On the other hand, there is a push towards ever higher data rates, whether via gateways or direct user access. At the same time, there is a trend towards heterogeneous networks supporting a wide range of end-to-end broadband communication services. These trends drive system design. Simpler orbital constellations and fewer satellites translate into lower system cost but lead to the need for more focused coverage, as opposed to worldwide coverage. The Quality-of-Service (QoS) provided is dependent on factors including the system, channel, radio and the availability and mechanisms for sharing of resources. Substantially more spectrum resources are available in EHF than in lower frequency bands, but ever higher data rates and increasing numbers of users competing for these resources places greater demands on mechanisms for efficient sharing of satellite resources (i.e., bandwidth and power) in terms of both hardware and software. This drives complexity and cost up. Further, integration into heterogeneous terrestrial networks (e.g. fiber, cable, wireless) may require adaptation at multiple levels of the protocol stack, from physical layer rate conversion to link and network layer protocol conversion.

The integration of satellite systems with the internet must take the capabilities and limitations of TCP/IP into account. New QoS features provided by IPv6 (e.g. flow labels, mobility support) facilitate broadband and mobile networks. However, issues today considered solved must be revisited when it comes to data rates on the order of 1 Gbps. Limitations of TCP/IP over satellite (e.g. the sliding window mechanism, available memory per connection, slow start and routing) are well known [75-82]. Key issues include the bandwidth-delay product, slow start, congestion control, acknowledgement and error recovery mechanisms [79-82]. These issues have been

investigated and various solutions have been proposed including TCP acknowledgement windows [79], larger initial window sizes to mitigate the problem of slow start [82], support for multiple QoS classes [83] and differential service [84]. The performance of TCP/IP over satellite is also sensitive to errors and the Q-V band and W band channel impairments must be considered.

Today, an industry standard for IP over Satellite (IPoS) exists [85-87]. IPoS separates satellite-specific aspects from satellite-independent higher layers, which facilitates future IP-based networking developments and terminal updates. Gbps data rates break new ground though. The capabilities and limitations of TCP/IP and other protocols over satellite links will need to be revisited. For example (see Fig. 13), in the case of TCP/IP, especially over long delay GEO satellite links, the delay-bandwidth product may become extremely large (e.g. 1 Gbps x 0.5 seconds Round Trip Time = 500 Mbits) far exceeding the currently available TCP window size (16 bits, 65536 octets or 524288 bits). This is before consideration of the channel and errors and, as can be seen from figure 13, a large window size (TCP scale option) does not necessarily help.

C. Emerging technologies and their potential impact

Ultra high data rate applications and services, especially to small and mobile ground terminals, place heavy demands on the satellite payload and terminals. Gbps data rates are one or more orders of magnitude beyond what is offered today (future broadband EHF communication satellites will require much more powerful payloads than today). High performance favors regenerative payloads employing e.g. on-board processing (OBP), Software Defined Radio (SDR) and beam-forming to optimize performance and efficiently use available spectrum and power resources. The tradeoff is between payload performance and flexibility on the one hand and mass, power and cost on the other hand.

SATCOM transponders may be categorized as “bent-pipe” or “processed”. The advantages of the bent-pipe transponder are that it is simple and low cost. It is basically an amplifier in the sky and transparent to the transmitted signal. By comparison, a processed satellite transponder regenerates the received signal. This requires reception of the signal (i.e., demodulate, detect, decode), not only amplification, before it can then be regenerated and retransmitted. The advantage is in flexibility.

Another potentially important advantage of a processed satellite concerns networking. Internet routing requires reading of packet headers. This can

only be done when the signal is fully demodulated, detected and decoded. RF switching and routing are of course possible but do not offer the same capability. Clearly, processed satellites offer advantages for “Internet-in-the-sky” systems, such as envisioned for Teledesic. Regenerative payloads are not new and standards exist [70][87], but multi-standard, SDR-based solutions for SATCOM remain in the future.

Radio-Frequency MEMS (RF-MEMS) are expected to offer the best performance at frequencies above 10 GHz, potentially replacing conventional components [88]. Lighter weight is not the only advantage offered by MEMS. A comparison with other switching technologies is provided in Table 4 [88-89]. For this reason, dynamic beam-forming and resource allocation remain in the future. However, reliability and switching speed are expected to be sufficient for offering reconfigurability (e.g. for coverage area) in the near-to-mid-term [90-92].

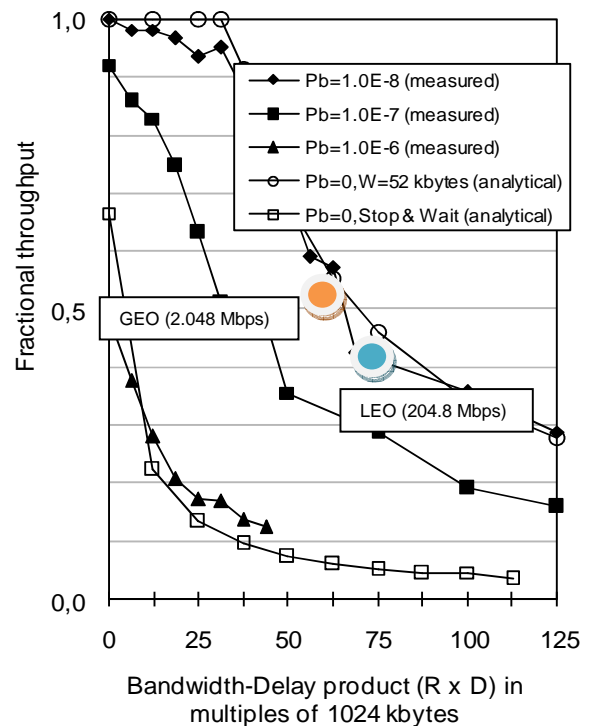


Fig.13. Fractional throughput of a TCP/IP carrier as a function of the delay-bandwidth product in multiples of 1024 kbytes, one-way delay (D) in seconds \times data rate (R) in bps, Window size limit = 51 \times 1024 bytes per TCP connection (51 blocks \times 1024 byte s/blocks \times 8 bits/byte), $R \times D = 62.5 \times 1024$ kbytes corresponds to a 2.048 Mbps carrier \times 0.25s one-way delay (GEO link, 38000km), $R \times D = 75 \times 1024$ kbytes corresponds to a 204.8 Mbps carrier \times 0.0033s one-way delay (LEO link, 1000km)

Tab. 3. EHF and Broadband SATCOM systems

System	Date	Orbit	Altitude (km)	Band	Network	Capacity	Services
Astrolink (Lockheed/Martin)	2003	9 GEO	36000	Ka-band	IP/ATM ISDN	6.5 Gbit/s	High-speed multimedia
CyberStar (Loral)	2001	3 GEO	36000	Ka-band	IP/ATM Frame relay	9.6 Gbit/s	Internet access, VoD broadband services
Eutelsat (Tooway)	2010	GEO	36000 (Hotbird 6 Ka Eurobird 3 Ku)	Ka-band Ku-band	8 hub terrestrial net interconnected via MPLS Internet backbone.	70.0 Gbps Up to 2M users DL up to 10Mbps, UL up to 1 Mbps.	Broadband Internet access
Hylas 1-2 (Avanti, Hughes, Orbital Sciences)	2010-2012	GEO	36000	Ka-band	IP based	8280MHz (Hylas2) 3000MHz (Hylas1) 24 Ka-band user beams and 6 gateway beams	Direct Broadcasting to homes (e.g. video), bi- directional communication, high-speed data (e.g. corporate networking) and broadband Internet.
O3b (Google, SES)	2009	8 MEO	8063 km	Ka-band	IP trunking	10 beams, 1.2 Gbps per beam	Ultra low latency IP backhaul services, next generation VSAT connectivity, world coverage
SkyBridge (Alcatel)	2001	64 LEO (Walker)	1469	Ku-band	IP/ATM	> 20 M users	High-bit rate Internet access, interactive multimedia service
Spaceway (Hughes)	2002	16 GEO 20 MEO	36000 10352	Ka-band	IP/ATM ISDN Frame relay	>10 Gbit/s (present) 16/30 Mbps (UL/DL)	High-speed Internet, multimedia, DVB, VSAT. Regenerative payload (TIA/ETSI standard), Spaceway 3 launch 8/07
Teledesic (Microsoft)	2002	288 LEO 12 planes of 24	1375	Ka-band 60 GHz	IP/ATM ISDN	10.0 Gbit/s	"Internet-in-the-Sky", high quality voice, data, video
Telesat	2004	GEO	36000 (Telesat Anik F2)	Ka-band Ku-band C-band	IP based	38 Ka, 32 Ku and 24 C-band transponders	Two-way, high-speed Internet services for consumers and businesses in rural and remote areas
WildBlue (ViaSat)	2004	2 GEO	36000 (Telesat Anik F2)	Ka-band	IP based	DL 1.5 Mbps UL 256 kbps	High-speed, two-way satellite Internet services

Tab.4. A comparison of switch technologies

Figure of Merit	PIN Diodes	GaAs FETs	MEMS switches
Isolation	Good	Good	Excellent
Insertion loss	Good	Good	Excellent
Power handling	Good	Poor	Excellent
Power consumption	Poor	Good	Excellent
Switching speed	Good	Excellent	Poor
Cost	Good	Poor	Good

6. ON-GOING AND FUTURE PLANNED EHF SATELLITE SCIENTIFIC EXPERIMENTS AND OPERATIONAL SYSTEMS

Ka band (27-40 GHz) can be considered as the current emerging standard for satellite communication systems while there are a good number of systems,

most of them are for dual-use (civil and defence) applications, operating in Q/V band (40-75 GHz). In this section a background on EHF broadband satellite systems state of the art is provided, focusing the attention on "beyond-Ka" ones, together with an overview on the most important planned and operative EHF broadband missions using the Q-V band and W-band (76-110 GHz) which considers the main international actors working in the field.

6.1 Q/V-band Systems

A. ITALSAT Missions

ITALSAT F1 and F2 [93-94] are two experimental/pre-operative telecommunications GEO satellite built by Alenia Spazio for the Italian Space Agency (ASI). The first satellite, F1, was launched in January 16th 1991, the second one, F2, was launched in August 8th 1996. They provided 30 GHz (uplink) and 20

GHz (downlink) Italian domestic coverage using six high-directivity spot beams and a "global" national elliptic beam. The F1 spacecraft also carried sophisticated propagation beacons at 40 and 50 GHz, able to provide important information about satellite channel propagation in EHF bands. The propagation package included a telemetry-modulated 20 GHz beacon (also used for tracking), a 40 GHz beacon phase modulated by a 505 MHz coherent sub-carrier, and a polarization-switched (but otherwise unmodulated) 50 GHz beacon. It supports attenuation and depolarization measurements at 20, 40, and 50 GHz, as well as measurements of phase and amplitude dispersion. The propagation beacons had total European coverage; these beacons provided a unique opportunity to obtain propagation data appropriate for the next generation of 40/50 GHz systems. As a matter of fact the scientific results achieved through ITALSAT, in the field of satellite propagation channel characterization, are of paramount importance, being used for the creation of statistical models for atmospheric impairments (rain, clouds, gas, scintillation, etc.) in EHF.

B. Sicral System

Sicral 1 and 1B (Sistema Italiano per Comunicazioni Riservate ed Allarmi) are the first Italian satellites for secure tactical military communication over national and international areas and for mobile communication with earth, naval, and aerial platforms [95]. Sicral 1 is Europe's first mission exploring extremely high-frequency (EHF) broadcast frequencies. The system is in service since May 2001 and operates in three frequency bands (multi-payload and multi-transmission): EHF (20-44 GHz) for infrastructural communications, UHF (260-300 MHz) for mobile tactical communication, SHF (7-8 GHz), the main band for high volume data transfer, with a multi-beam reconfigurable antenna. The Sicral system is based on innovative technologies that enable the satellite to adapt promptly to changing emergency conditions. It is also highly flexible, with a large capacity and can be used for land, sea and air operations.

C. Alphasat "Technological Demonstration Payload #5" Mission

The European Space Agency (ESA) is developing a satellite platform named Alphasat [96]. This platform will be capable of carrying a payload of about 1000 kg with power consumption up to 16 kW. The Alphasat platform will be ready for launch in early 2012.

The primary objective of ESA under the Alphasat Program is to facilitate an early first flight, and in-orbit validation of the Alphasat platform. ESA will use this platform to offer operators, service providers and industrial groups the possibility to fly their payloads on board of the Alphasat proto-flight model.

ESA has selected the Inmarsat Global Ltd geomobile mission for the first flight opportunity (the program will be funded both by ESA and Inmarsat).

The Alphasat platform represents a unique opportunity for demonstrating new technologies, systems and services in-orbit so, in addition to the operational payload; ESA is also providing four Technology Demonstration Payloads (TDPs) for embarkation on the Alphasat. Among these payloads, the experimental TDP#5, named "Q/V band payload", will be devoted to the experimentation of Q/V band satellite propagation and communication [97-98]. The main goals of the Q/V Band TDP#5 mission are:

- to establish the effectiveness of ACM as propagation impairments mitigation technique in very high frequency band operation (ACM implementation as defined in the DVB-S2 standard will be used in the experiments);
- to test and establish the effectiveness of other PIMT, complementary to ACM, like:
 - site diversity,
 - up-link power control;
- to improve the knowledge of propagation impairments at Q/V band which is a fundamental step for the design of satellite communication systems adopting adaptive techniques, e.g. ACM, on-board antenna pattern re-configurability, up- and down-link power control. In particular, a better characterization of 2nd-order statistics is currently required to better exploit the characteristics of the new interference and fading mitigation schemes, like the one just mentioned;
- test the technologies required for implementing a modern communication payload in Q/V band, verifying in-flight performance of innovative hardware.

The system will be capable to establish and maintain full-duplex communication links between the reference landing point located in Tito (Italy) and:

- a site located in Northern Italy (reference landing point: Spino d'Adda),
- a site located in Central Europe (reference landing point: Graz, Austria).

The space to Earth communication will be performed in the Q band region while the Earth to space communication will be performed in the V band region.

D. MILSTAR System

The Milstar (Military Strategic and Tactical Relay) system is a tactical and strategic multi-service program involving the U.S. Air Force, Army, Navy, and other agencies [99-100]. Milstar is in service since 1994 and provides protected communications for command and control of the United States war-fighting forces (including the National Command Authority, military tactical and strategic forces, Air Force Space Command

and other users). Milstar is a constellation of GEO satellites that provides uplink communications at EHF, 44 GHz, and UHF, 300 MHz, and downlink communications at SHF, 20 GHz, and UHF, 250 MHz. It provides survivable medium data rate (MDR, in the range from 4.8 kbps to 1.5 Mbps), at 44 GHz uplink and 20 GHz downlink, and low data rate (LDR, at 2.5 kbps) communications services between terminals worldwide using cross-links between Milstar satellites (both for the MDR and LDR payloads) operating in the 60 GHz region. Survivability and endurance requirements are satisfied by anti-jam, low probability of interception and detection (guaranteed by the use of EHF), hardening and system autonomy features.

E. AEHF System

The AEHF (Advanced Extreme High Frequency Satellite) program [99-100] will be the follow-on to the Milstar system providing the military's next generation of highly secure strategic and tactical communications satellites. AEHF is currently under development and will become the protected backbone of the U.S. Department of Defense's military satellite communications architecture.

The AEHF system will be backward compatible with Milstar's low data rate and medium data rate capabilities, while providing extreme data rates (XDR) and larger capacity. The higher data rate modes will provide data rates up to 8.2 Mbps to future Advanced EHF Army terminals (the system will be able to support 6000 terminals). Each Advanced EHF satellite employs more than 50 communications channels via multiple, simultaneous downlinks. For global communications, the Advanced EHF system will use inter-satellite cross-links. The higher data rates permit transmission of tactical military communications such as real-time video, battlefield maps and targeting data.

F. COMETS System

The COMETS (Communication and Broadcasting Engineering Test Satellite) project was jointly developed by NASDA (National Space Development Agency, at present JAXA, Japan Aerospace Exploration Agency) and the Ministry of Post and Telecommunications / Communications Research Laboratory (MPT/CRL) [101-102]. COMETS was developed to evaluate Ka-band (31/21GHz) and millimeter-wave (47/44GHz) advanced mobile satellite communications systems, 21-GHz advanced satellite broadcasting systems, and S-band and Ka-band inter-orbit satellite communications systems.

Unfortunately in 1998 the launch failed and the satellite could not reach geostationary orbit (and became an elliptic orbit system). Anyhow some propagation measurements for land mobile satellite communications channels at Ka/Q-band have been

performed; shadowing effects in land-mobile satellite channels due to roadside telegraph poles and electric wires were measured in the urban area of Tokyo and in Sydney, in the Ka band (21GHz) and millimeter wave band (44GHz). COMETS terminated its operations in 1999.

6.2 W-band Systems

Currently no operative W band satellite communication system has been developed. The W band can certainly be considered as a frontier for space telecommunication applications. Anyhow there are some missions in the development phase conceived to perform telecommunication links in the W-band; in the following sections the main characteristics of these missions are reported and analysed.

A. DAVID Mission

DAVID (DATA and Video Interactive Distribution) is a satellite scientific mission of the Italian Space Agency (ASI) [103-104]. Currently the B phase of the DAVID Mission has been completed and the C/D proposal has been delivered to ASI. The DAVID satellite is planned to be located in a Sun-synchronous low earth orbit at about 570 km, ensuring the re-visitation of the same sites at the same hour every day. The DAVID mission is composed of two main experiments, which aim at:

- exploring the W-band channel for high capacity data transfer (Data Collection Experiment, DCE);
- test dynamic resource sharing techniques (Resource Sharing Experiment, RSE) for the optimal exploitation of the extremely high frequency satellite channel.

The Data Collection Experiment aim is to prove the feasibility of high-speed data collection from a content provider station via a W-band link at 84.5 GHz. Since this frequency band is still unused for satellite communications, a large portion of the spectrum is available, leading to the possibility of collecting data at about 100 Mbit/s practically "error free" (BER of the order of 10^{-11}), and so allowing to upload on the on-board memory at least 1 Gbyte of net data during the short visibility time window of each passage over the content provider station locations.

B. WAVE Project

WAVE (W-band analysis and VERification) project is an ASI project, follow-on of the previously described DAVID mission; WAVE has been conceived with the goal to make possible the deployment of operative LEO/GEO satellite in the W-band for commercial use in 15 years. More specifically, the WAVE-A2 project aims at designing and developing a complete line of W-band communication satellite payloads [105-106]. Currently the project A2 phase has been satisfactorily concluded. The project includes two demonstrative missions and

two pre-operative missions. The demonstrative missions are needed to characterize the channel and test the technology in-orbit:

- Aero-WAVE mission, which is based on COTS (Commercial Off-the-Shelf) hardware and High altitude Platform, will give preliminary results for the channel characterization;
- the IKNOW (In-orbit Key test and validation of W-band) mission, based on a small LEO, which will be the first W-band telecommunication satellite mission, that will provide first order statistics of satellite channel additional attenuation.

The two pre-operative missions, one over a LEO and the other one over a GEO, which will employ the results achieved from the demonstrative missions and will be used to perform preliminary tests for the commercial/operative use of the W-band.

C. The Quasi-Zenith Satellite System

This JAXA project is a feasibility study for a 3 Geosynchronous satellite constellation, each satellite has 45° of inclination; through this constellation it is possible to obtain a near-continuous coverage over Japan and Australia with a quasi-zenithal elevation angle (greater than 70°) [107]. The system will be used as an augmentation of the Global Positioning Service and as backbone for VSAT-VSAT links, as secondary service.

The proposed operative frequencies for TLC application are 84 GHz and 74 GHz, for uplink and downlink respectively; the system will provide a data rate of 45 Mbps (allowing the coverage of Polar Regions). This satellite system provides good propagation performance for what concerns urban mobile telecommunication services; in fact, having an elevation angle greater than 70°; it allows a strong reduction of the shadowing in metropolitan areas.

D. Use of W-band in the Integrated Interplanetary Network

NASA and other Space Agencies are involved in the design of a space infrastructure able to support the future solar system exploration missions, both manned and unmanned; this infrastructure will be able to relay data from landers, satellites, rovers, etc. to the Earth. This infrastructure is called Integrated Interplanetary Network (IIN), it will consist of a fleet of data relay satellites positioned through the solar system to support space exploration activities [108].

The IIN will be gradually deployed, positioning the first two key nodes, the Data Relay Satellites (DRS), around Earth and around Mars. A telecommunication infrastructure will be developed around Mars in order to provide data relay and navigation services. The space network will be developed adding other satellites that

can be considered as communication nodes, as additional needs arise.

The IIN requires great technology development that can support the transfer of high volumes of scientific and communication data. In this framework the W band can be considered as a key enabling technology for ISL links between space nodes of the infrastructure, due to the absence of additional atmospheric attenuation; W band will be useful in order to realise reliable, high bandwidth, space trunk lines.

7. CONCLUSIONS

This paper presented an overview about the current research activities dealing with the use of Extremely High Frequencies (EHFs) for broadband satellite communications. The potential advantages deriving from the transmission of satellite data in the millimeter wave domain have been known for years. The frequency bands that are more favorable to satellite applications (i.e.: Q-V and W) have already been individuated by the theoretical studies about EHF atmospheric propagation. But, as usual, the passage from theoretical appraisal to technological development is not so straightforward.

The open problems are mostly related to the uncertainties about the effects of rain and clouds on a real transmission. Models available in literature are based on theoretical/mathematical evaluations and extensions to higher frequencies of attenuation series available at lower frequencies. The lesson learnt in 60 years of satellite communications says that only a real measurement done by a probe can guarantee a reliable appreciation of atmospheric effects. This will be the first, essential, task in charge to on-going and future EHF satellite missions. Anyway, it is expected that the strong atmospheric attenuation may limit the link availability to 95% or even less. The question is how much can this value be increased by means of PIMPT techniques or site diversity.

Another open issue is related to the PHY-layer design that should be able to work in the presence of saturating amplifiers (without wasting power in back-off operations that are not welcome) and relevant amounts of phase-noise. The tradeoff to be solved is related to the necessity of incrementing spectral efficiency without increasing demodulation losses due to uncompensated distortions or phase jitters. In such a perspective, valuable solutions may come from advanced PHY-layer design mainly based on innovative pulse shaping, adaptive modulation and coding (AMC), trellis-coded and turbo-trellis-coded modulations. The adoption of multicarrier modulations in the EHF framework is promising but still to be assessed.

Considering networking and application aspects, it is clear that primary services that could be supported by EHF satellite systems include two-way, high-speed Internet access at rates of 100 Mbps to 1 Gbps as well as VSAT business services and direct broadcast to homes. Support for ever more resource demanding services requires not only bandwidth; it also requires increasingly powerful satellite payloads. Optimization of the payload to support a wide range of applications, networks, regions and changing traffic environments places greater demand on signal processing and reuse of resources. Reconfigurability will be increasingly important. This includes not only modulation and coding, but also antenna beams, coverage regions and frequency bands – towards a reconfigurable payload for broadband access.

What is the “killer application” for such a high performance future broadband satellite? In a broadband SATCOM system integrated with heterogeneous terrestrial networks and targeting Gbps data rates, the ability to flexibly and efficiently allocate resources when and where they are needed is a must in order to provide

SATCOM customers and end users with the services that they have come to expect (e.g. high-speed Internet access) transparently and cost competitively.

In order to practically provide to users this augmented Quality-of-Service, efficient mechanisms of radio resource management (bandwidth and power), that will work in the presence of an increasing number of competing users, should be studied. Maybe higher-layer protocols would also need a revision, taking into account the necessity of supporting ultra-high data rates and, therefore, to boost network throughput. In such a perspective, regenerative payloads based on reconfigurable Software-Defined-Radio technologies should play a key role.

8. ACKNOWLEDGMENTS

Authors wish to thank Dr. Vittorio Dainelli of Rheinmetall Italia S.p.A. (Italy) for the data about real W-band hardware devices kindly provided to them.

REFERENCES

- [1] M. Ibnkahla, Q.M. Rahaman, A.I. Sulyman, H. Al-Asady, J. Yuan, and A. Safwat, “High-Speed Satellite Mobile Communications: Technologies and Challenges”, *Proc. IEEE*, vol.92, no.2, Feb. 2004, pp.312-339.
- [2] J. Farserotu, and R. Prasad, “A Survey of Future Broadband Multimedia Satellite Systems, Issues and Trends”, *IEEE Comm. Mag.*, June 2000, pp. 128-133.
- [3] W.E. Morrow, “Scanning the Issue”, *Proc. IEEE, Spec. issue on Satellite Communications*, vol.59, no.2, Feb. 1971, pp. 116-117.
- [4] R. K. Crane: “Propagation phenomena affecting satellite communication systems operating in the centimeter and millimeter wavelength bands”, *Proc. IEEE*, vol.59, no.2, Feb. 1971, pp. 173-188.
- [5] L. J. Ippolito: “Radio propagation for space communication systems”, *Proc. IEEE*, vol. 69, no. 6, Jun. 1981, pp. 697-727.
- [6] H. J. Liebe: “Atmospheric EHF window transparencies near 35, 90,140 and 220 GHz”, *IEEE Trans. on Antennas and Propagat.*, vol. 31, no.1, Jan. 1983, pp. 127-135.
- [7] E. Cianca, M. Ruggieri, and A. Paraboni, “Experimental Aerospace Missions for EHF Communications”, *Proc. of 1st IEEE EHF-AEROCOMM Workshop*, New Orleans (LA), 30 Nov. 2008, pp.1-6.
- [8] R.A. Bohlander, and R. W. McMillan: “Atmospheric effects on near millimeter wave propagation”, *Proc. IEEE*, vol.73, no.1, Jan. 1985, pp. 49-60.
- [9] H. J. Liebe: “An updated model for millimeter wave propagation in moist air”, *Radio Science*, vol. 20, no.5, May 1985, pp. 1069-1089.
- [10] H. J. Liebe: “MPM – An atmospheric millimeter-wave propagation model”, *Int. J. of Infrared and Millimeter waves*, vol.10, no.6, June 1989, pp. 631-650.
- [11] H. J. Liebe, T. Manabe, and G. A. Hufford: “Millimeter-wave attenuation and delay rates due to fog / cloud conditions”, *IEEE Trans. on Antennas and Propagat.*, vol. 37, no.12, Dec. 1989, pp. 1617-1623.
- [12] H. J. Liebe, G. A. Hufford, and T. Manabe: “A model for the complex permittivity of water at frequencies below 1THz”, *Int. J. of Infrared and Millimeter Waves*, vol. 12, no.7, July 1991, pp. 659-675.
- [13] Y. Pinhasi, A. Yahalom, O. Harpaz, and G. Vilner: “Study of ultra wideband transmission in the extremely high frequency (EHF) band”, *IEEE Trans. on Antennas and Propagat.*, vol. 52, no.11, Nov. 2004, pp. 2833-2842.
- [14] Y. Pinhasi, and A. Yahalom “Spectral Characteristics of Gaseous Media and Their effects on Propagation of Ultra-Wideband Radiation in the Millimeter Wavelengths”, *J. Non-Cryst. Sol.*, vol. 351, no. 33-36, 15 Sept. 2005, 2925-2928
- [15] Y. Pinhasi, A. Yahalom, and G. A. Pinhasi: “Propagation Analysis of Ultra-Short Pulses in Resonant Dielectric Media”, *J. Opt. Soc. Am. B*, vol. 26, no. 12, Dec. 2009, pp. 2404-2413.
- [16] ITU-R P.618, “Propagation data and prediction methods required for the design of Earth-space telecommunication systems”.
- [17] J.D. Laster, and W.L. Stutzman, “Frequency scaling of rain attenuation for satellite communication links”, *IEEE Transactions on Antennas and Propagat.*, vol.43, no. 2, Nov 1995, pp.1207-1216.
- [18] “*Handbook on Satellite Communications*”, edited by International Telecommunication Union (ITU), 3rd edition, Wiley, New York (NJ): 2002.
- [19] G. Maral, and M. Bousquet, “*Satellite Communication Systems*”, 3rd edition, Wiley, New York (NJ):1998.
- [20] S. De Fina, M. Ruggieri, A. V. Bosisio, “Exploitation of the W-band for High-Capacity Satellite Communications”, *IEEE Transactions on AES*, vol. 39, no. 1; January 2003, pp. 82-93.
- [21] C. Sacchi, G. Gera, and C. Regazzoni, “W-band Physical Layer Design Issues in the Context of the DAVID-DCE Experiment”, *Int. Jour. of Satellite Communications and Networking*, vol. 22, no. 2, March-April 2004, pp. 193-215.
- [22] W.L. Martin, and T.M. Nguyen, “*CCSDS-SFCG Efficient Modulation Methods Study: A comparison of Modulation Schemes, Phase 2: Spectrum Shaping*”, CCSDS Tech. Rep. August 1994.
- [23] J.L. Fikart, and B. Kocay, “Cost Effective Operating Power Specification of Ka-Band MMICS for Multimedia Satellite Interactive Terminals”, *Proc. of 1999 IEEE MTT-S Symp. on Tech. for Wireless Appl.*, 21-24 Feb. 1999, pp. 247-252.
- [24] M. Blank, B.G. Danly, and B. Levush, “Circuit Design of a Wideband W-Band Gyroklystron Amplifier for Radar Applications”, *IEEE Trans. on Plasma*

- Science*, vol.26, no.3, June 1998, pp. 426-432.
- [25] A.J. Theiss, C.J. Meadows, R.B. True, and J.M. Martin, "High-Average-Power W-band TWT Development", *IEEE Trans. on Plasma Science*, vol.38, no.6, June 2010, pp. 1239-1243.
- [26] B. Wicks, E. Skafidas, and R. Evans, "A 75-95 GHz Wideband CMOS Power Amplifier", *Proc. of 1st European Wireless Tech. Conf. (EuMA 2008)*, Amsterdam (NL), 27-31 Oct. 2008, pp. 230-233.
- [27] A. Jacquez, and G. Wada, "44 GHz Helix TWTs for Satellite Communications", *Proc of 1986 IEEE Electron. Dev. Meeting*, Los Angeles (CA), 7-10 Dec. 1986, vol. 32, pp.501-504.
- [28] C. Sacchi, T. Rossi, M. Ruggieri and F. Granelli, "Efficient Waveform Design for High-Bit-Rate W-band Satellite Transmissions", *IEEE Trans. on AES*, vol.47, no.2, April 2011, pp. 974-995.
- [29] G. Satoh, and T. Mizuno, "Impact of a New TWTA Linearizer Upon QPSK/TDMA Transmission Performance", *IEEE J. on Selec. Areas in Comm.*, vol.SAC-1, no.1, Jan. 1983, pp. 39-45.
- [30] A. Katz, R. Gray, and R. Dorval, "Wideband/Multiband Linearization of TWTAs Using Predistortion", *IEEE Trans. on Electron Devices*, vol.56, no.5, May 2009, pp. 959-964.
- [31] T.H. Lee, and A. Hajimiri, "Oscillator Phase Noise: A Tutorial", *IEEE J. of Solid-State Circuits*, vol.35, no.3, March 2000, pp. 326-336.
- [32] R. Strangeway, T. Koryu-Ishii, and J.S. Hide, "Low-Phase-Noise Gunn Diode Oscillator Design", *IEEE Trans. on Microwave Theory and Techniques*, vol.36, no.4, April 1988, pp.792-794.
- [33] G.M. Smith and J.C.G. Lesurf, "Stabilization of Millimeter Wave Oscillators", *Proc. of IEE Colloquium on Characterization of Oscillators and Measurement*, London (UK), 1992, pp. 6/1-6/5.
- [34] B. Jingfu, H. Songbai, S. Yue, and W. Yu, "Low Noise W-band Phase Locked Loops", *Proc. of 1997 IEEE Asia Pacific Microwave Conf.*, pp. 321-323.
- [35] Z. Yonghong, T. Xiaohong, and F. Zhenghe, "The investigation of W-band solid-state frequency sources", *Proc. of 2003 3rd Int. Conf. on Microwave and Millimeter Wave Tech.*, pp. 1125-1128.
- [36] J.K. Holmes, "Coherent Spread Spectrum Systems", Wiley, Chichester (UK): 1981.
- [37] J.R. Alexovich, and R.M. Gagliardi, "The Effect of Phase Noise on Noncoherent Digital Communications", *IEEE Trans. on Comm.*, vol.38, no.9, Sept. 1990, pp. 1539-1548.
- [38] H. Ma, and X. Tang, "Study on W-band PLL Frequency Synthesizer for Space Communications", *Proc. PIERS*, Hangzhou, China, March 24-28, 2008, pp. 342-345.
- [39] S. O. Tatu, E. Moldovan, G. Brehm, K. Wu, R. G. Bosio, "Ka-Band Direct Digital Receiver" *IEEE Trans. on Microwave Theory and Techniques*, Vol. 50, No. 11, Nov. 2002, pp.2436-2442.
- [40] X. Huang, "A direct conversion receiver for satellite communication systems", *Int. J. of Satellite Comm. and Networking*, Vol. 23, No. 2, March-April 2005, pp. 129-141.
- [41] C. Sacchi, M. Musso, G. Gera, C. Regazzoni, F.G.B. De Natale, A. Jebril, and M. Ruggieri, "An Efficient Carrier Recovery Scheme for High-Bit-Rate W-Band Satellite Communication Systems", *Proc. of 2005 IEEE Aerospace Conf.*, Big Sky, (MT), 5-12 March 2005, available on CD-ROM.
- [42] S. Benedetto, M. Mondin, and G. Montorsi, "Performance Evaluation of Trellis-Coded Modulation Schemes", *Proc. IEEE*, vol. 82, no. 6, June 1994, pp. 833-855.
- [43] C. Sacchi and A. Grigorova, "Use of Trellis-Coded Modulation for Gigabit/sec Transmissions over W-Band Satellite Links", *Proc. of 2006 IEEE Aerospace Conf.*, Big Sky (MT), 4-11 March 2006, available on CD-ROM.
- [44] R. El-Awadi, M.A. Bahie Eldin, L.F. Gergis, "Performance of Concatenated Turbo-Trellis Coded Modulation for Mobile Satellite Channels", *Proc. of 18th National Radio Conf.*, Mansoura (Egypt), 27-29 Mar. 2001, pp. 369-377.
- [45] P.A. Martin, M.A. Ambroze, D.P. Taylor, and M. Tomlinson, "Coding for Shared Satellite Channel Communications", *IEEE Trans. on Comm.*, vol.57, no.8, Aug. 2009, pp. 2330-2338.
- [46] S.L. Howard, and C. Schlegel, "Differential Turbo-Coded Modulation with APP Channel Estimation", *IEEE Trans. on Comm.*, vol.54, no.8, Aug. 2006, pp.1397-1405.
- [47] M. Rice, T. Oliphant, O. Haddadin, and W. McIntire, "Estimation Technique for GMSK using Linear Detectors in Satellite Communications", *IEEE Trans. on AES*, vol.43, no.4, Oct. 2007, pp. 1484-1495.
- [48] K. Usuda, H. Zhang, and M. Nakagawa, M-ary pulse shape modulation for PSWF-based UWB systems in multipath fading environment, *Proc. 2004 IEEE Globecom Conf.*, Dallas (TX), 29 Nov. - 3 Dec. 2004, pp. 3498-3504.
- [49] Digital Video Broadcasting (DVB), "Second generation framing structure, channel coding and modulation systems for Broadcasting, Interactive Services, News Gathering", DVB-S2 draft document DVBS2-74, June 2003.
- [50] R. De Gaudenzi, A. Guillen-Fabregas, A. M. Vicente, and B. Ponticelli, "High Power and Spectral Efficiency Coded Digital Modulation Schemes for Non-linear Satellite Channels", *Proc. of 7th Int. ESA Workshop on Digital Signal Proc. Tech. for Space Appl.*, Sesimbra (P), Oct. 2001.
- [51] L. Giugno, V. Lottici, and M. Luise, "Adaptive Compensation of Non-linear Satellite Transponder for Uncoded and Coded High-Level Data Modulations", *IEEE Trans. on Wireless Comm.*, vol.3, no.5, Sept. 2004, pp. 1490-1495.
- [52] G. Karam and H. Sari, "A Data Predistortion Technique with Memory for QAM Radio Systems", *IEEE Trans. on Comm.*, vol. 39, no. 2, Feb. 1991, pp. 336-344.
- [53] C. Berrou, et. al., "High Speed Modem Concepts and Demonstrator for Adaptive Coding and Modulation with High Order in Satellite Applications", *Proc. of ESA Conf. on Signal Proc. for Space Comm. (SPSC)*, Catania (I), 23-25 Sept. 2003, http available.
- [54] L. Castanet, A. Bolea-Alamanac, and M. Bousquet, "Interference and fade mitigation techniques for Ka and Q/V band satellite communication systems", *Proc. of Int. Workshop on Satellite Comm. from Fade Mitigation to Service Provision*, Noordwijk (NL), May 2003.
- [55] S. Mukherjee, M. De Sanctis, T. Rossi, E. Cianca, M. Ruggieri, R. Prasad, "On the Optimization of DVB-S2 Links in EHF Bands", *Proc. of 2010 IEEE Aerospace Conf.*, Big Sky (MT), 6-13 March 2010, available on CD-ROM.
- [56] Y. Nakasha et. al., "A W-band Wavelength Generator using 0.13 μm InP HEMTs for Multigigabit Communications Based on Ultra-Wideband Impulse Radio", *Proc. of 2008 IEEE Int. MTT-S Symp.*, Atlanta (GA), June 15-20 2008, pp. 109-112.
- [57] C. Stallo, S. Mukherjee, E. Cianca, T. Rossi, M. De Sanctis, and M. Ruggieri, "On the Use of UWB Radio Interface for EHF Satellite Communications", *Proc. of 2010 IEEE Aerospace Conf.*, Big Sky (MT), 6-13 March 2010, available on CD-ROM.
- [58] A. Papatthanassiou, A. Salkintzis, and P. Mathiopoulos, "A Comparison Study of the Uplink Performance of W-CDMA and OFDM for Mobile Multimedia Communications via LEO Satellites", *IEEE Pers. Comm.*, Jun. 2001, pp. 35-43.
- [59] S. Janaathanan, C. Kasparis, and B.G. Evans, "Comparison of SC-FDMA and HUSPA in the Return-Link of Evolved S-UMTS Architecture", *Proc. of 2007 Int. Workshop on Satellite and Space Comm.*, Salzburg (A), 13-14 Sept. 2007, pp. 56-60.
- [60] S. Cioni, G.E. Corazza, M. Neri, and A. Vanelli-Coralli, "On the Use of OFDM Radio Interface for Satellite Digital Multimedia Broadcasting Systems", *Int. J. of Satellite Comm. and Networking*, vol. 24, no. 2, March-Apr. 2006, pp. 153-167.
- [61] S. Cioni, G.E. Corazza, M. Neri, A. Vanelli-Coralli, "OFDM vs. HSDPA Comparison for Satellite Digital Multimedia Broadcasting Systems", *Proc. of 2005*

- IEEE Globecom Conf.*, St. Louis (MO), 28 Nov. - 2 Dec. 2005, vol. 5, pp. 2922-2926.
- [62] S. C. Thompson, A. U. Ahmed, J. G. Proakis, J. R. Zeidler, and M. J. Geile, "Constant Envelope OFDM", *IEEE Trans. on Comm.*, Vol. 56, no. 8. August 2008, pp. 1300-1312.
- [63] S. Suzuki, O. Takyu, and Y. Umeda, "Performance Evaluation of Effect of Nonlinear Distortion in SC-FDMA System", *Proc. of Int. Symp. on Inf. Theory and its Appl. (ISITA 2008)*, Auckland (NZ), Dec. 7-10, 2008, pp.1-5.
- [64] E. Elizondo, R. Gobbi and R. Modelfino, "Astrolink™ Satellite System Overview", *Proc. of 1998 IEEE Aerospace Conf.*, Big Sky (MT), 21-28 Mar 1998, vol.4, pp. 539 - 546.
- [65] *Eutelsat Tooway*, www.eutelsat.com/news/media_library/brochures/tooway.pdf
- [66] *Hylas 2 Commercial Satellite*, <http://www.aerospace-technology.com/projects/hylas-2-satellite/>
- [67] Lloyd's satellite constellations, <http://info.ee.surrey.ac.uk/Personal/L.Wood/constellations/teledesic.html>
- [68] O3b Networks, <http://www.o3bnetworks.com/>
- [69] P. Sourisse, D. Rouffet and H. Sorre, "SkyBridge: a broadband access system using a constellation of LEO satellites", [http available at: www.itu.int/newsarchive/press/WRC97/SkyBridge.html](http://www.itu.int/newsarchive/press/WRC97/SkyBridge.html)
- [70] *Spaceway*, <http://www.hughes.com/ProductsAndTechnology/spaceway/Pages/Spaceway.aspx>
- [71] *Teledesic*, <http://en.wikipedia.org/wiki/Teledesic>
- [72] *Telesat*, <http://www.telesat.ca/>
- [73] *WildBlue*, <http://www.wildblue.com/>
- [74] "Broadband Technology Overview", Corning, white paper, Optical Fiber, June 2005.
- [75] J. Farserotu and R. Prasad, "IP/ATM Mobile Satellite Networks", Artech House, London, UK, 2002.
- [76] L. Wood et. al, "IP Routing issues in Satellite Constellation Networks", *Int. J. of Satellite Comm.*, vol.19, no.1, Jan-Feb. 2001, pp. 69-92.
- [77] S. Kota, M. Goyal, R. Goyal and R. Jain, "Broadband satellite network: TCP/IP performance analysis", *Kluwer International Federation For Information Processing Series*, Vol. 159, pp. 273-282, 2000.
- [78] J. Farserotu and R. Prasad, "Wide Area Networking via ATM over Ka-band SATCOM with CDMA", *IEEE J. on Selec. Areas in Comm.*, vol. 17, no. 2, Feb. 1999, pp. 270-285.
- [79] V. Jacobson, R. Braden and D. Borman, "TCP Extensions for High Performance", RFC1323, proposed standard, May, 1992.
- [80] Mathis, J. Mahdavi, S. Floyd and A. Romanov, "TCP Selective Acknowledgement Options", RFC2018, proposed standard, October, 1996.
- [81] M. Allman, et. al., "Ongoing Research Related to Satellites", Network Working Group, RFC2760, February, 2000.
- [82] M. Allman, et. al., "Enhancing TCP Over Satellite Channels", Network Working Group, RFC2488, January 1999.
- [83] S. Blake, D. Black, et. al, "An Architecture for Differentiated Services", RFC2475, December 1998.
- [84] K. Nichols, et. al, "Definition of the Differentiated Services Field in the IPv4 and IPv6 Headers", RFC2474, December 1998.
- [85] "The IPOS Standard", Hughes Standards and Publications, [http available at: www.hughes.com](http://www.hughes.com)
- [86] U.S. Telecommunications Industry Association standard (TIA-1008), November 2003.
- [87] ETSI Broadband Satellite Multimedia (BSM) as defined in ETSI standard TR 101 984, [http available at: www.etsi.org/WebSite/Technologies/BroadbandSatMultimedia.aspx](http://www.etsi.org/WebSite/Technologies/BroadbandSatMultimedia.aspx).
- [88] Applied Research Road Maps for RF micro-nano systems Opportunities (ARRRO), proposal/contract N° 027752, 26/06/2007, D3.1: RF MEMS Roadmap, www.cordis.europa.eu
- [89] E. Chester, "CAE, Microsystem Integration Trends and Emerging Capabilities in the Space Sector", EURIPEDES presentation, Barcelona, 22 October 2009.
- [90] G. Rebeiz, "RF MEMS Theory, Design and Technology", John Wiley & Sons, NJ, USA, 2003.
- [91] B. Liu, "High Performance and Low Cost Capacitive Switches for RF Applications", U. California St. Barbara, Toyon Research, DARPA Frequency Agile Materials for Electronics.
- [92] T. Vaha-Heikkilä et.al, "RF MEMS Impedance Tuners for 6-24 GHz Applications", *Int. J. of RF and Microwave Computer-Aided Engineering*, May 2007, pp. 265-278.
- [93] R. Polonio, C. Riva, "ITALSAT propagation experiment at 18.7, 39.6 and 49.5 GHz at Spino D'Adda: three years of CPA statistics", *IEEE Transactions on Antennas and Propagat.*, vol. 46, no. 5, May 1998, pp. 631-635.
- [94] M. Mauri, A. Paraboni, A. Pawlina, "The OLYMPUS and ITALSAT propagation programs of the Italian Space Agency: an overview of the first experimental results in the 12 to 50 GHz frequency bands", *Proc. of 3rd European conf. on Satellite Comm.*, 2-4 Nov 1993, Pag. 263-268.
- [95] Italian Defence Department web site: <http://www.difesa.it/>
- [96] European Space Agency web site: <http://www.esa.int>
- [97] T. Rossi, et. al., "Experimental Italian Q/V Band Satellite Network", *Proc. of 2009 IEEE Aerospace Conf.*, Big Sky (MT), 7-14 March 2009, available on CD-ROM.
- [98] E. Cianca, et. al. "TRANSPONDERS: Effectiveness of Propagation and Impairments Mitigation Techniques at Q/V Band", *Proc. of 1st IEEE EHF-AEROCOMM Workshop*, New Orleans (LA), 30 Nov. 2008, pp.1-6.
- [99] U.S. National Security Space Road Map (NSSRM) web site: <http://www.fas.org/spp/military/program/nssrm/roadmap/dodprogs.htm>
- [100] U.S. Air Force web site: <http://www.af.mil/>
- [101] Y. Hase, "Propagation experiment of COMETS Ka/Q-band Communication Link for future satellite cellular system", *CRL publications*, vol. ACTS-95-029, 1995.
- [102] H. Wakana, H. Saito, S. Yamamoto, M. Ohkawa, N. Obara, H.-B. Li, and M. Tanaka, "COMETS experiments for advanced mobile satellite communications and advanced satellite broadcasting", *Int. J. of Satellite Comm.*, vol.18, no. 2, Apr. 2000, pp. 63-85.
- [103] C. Bonifazi, M. Ruggieri, A. Paraboni, "The DAVID mission in the heritage of the SIRIO and ITALSAT satellites", *IEEE Transaction on AES*, vol. 38, no. 4, Oct. 2002, pp.1371-1376.
- [104] M. Ruggieri, S. De Fina, M. Pratesi, A. Salomè, E. Saggese, C. Bonifazi, "The W-band Data Collection Experiment of the DAVID Mission", *IEEE Trans. on AES*, vol. 38, no. 4, Oct. 2002, pp. 1377-1387.
- [105] M. Lucente, T. Rossi, M. Ruggieri, A. Jebri, A. Iera, A. Molinaro, S. Pulitano, C. Sacchi, L. Zuliani, "Experimental Missions in W-Band: a Small LEO Satellite Approach", *IEEE Systems Journal*, vol.2, no.1, Mar. 2008, pp. 90-103.
- [106] M. Lucente, E. Re, T. Rossi, E. Cianca, C. Stallo, M. Ruggieri, A. Jebri, C. Dionisio, L. Zuliani, "IKNOW Mission: Payload Design for In Orbit Test of W Band Technology", *Proc. of IEEE Aerospace Conf. 2008*, Big Sky (MT), 1-8 March 2008, available on CD-ROM.
- [107] T. Takahasha, Y. Konishi, T. Noguchi, N. Futagawa, "Payload configuration study for Quasi Zenith Satellite System", *Proc. of 22nd AIAA Int. Conf. on Comm. Satellite Systems*, Monterey (CA), May 2004.
- [108] B. Younes, "White paper on Integrated Interplanetary Network (IIN)", NASA Publications and Reports, Nov. 2000.

AUTHORS' BIOGRAPHIES

Ernestina Cianca received the Laurea degree in Electronic Engineering "cum laude" at the University of L'Aquila in 1997. She got the Ph.D. degree at the University of Rome Tor Vergata (URTV) in 2001. She concluded her Ph.D. at Aalborg University where she has been employed in the Wireless Networking Groups, as Research engineer (2000-2001) and as Assistant Professor (2001-2003). Since Nov. 2003 she is Assistant Professor in Telecommunications at the URTV, teaching DSP, Information and Coding Theory and Advanced Transmission Techniques. She has been the principal investigator of the Italian Space Agency WAVE-A2 mission, aiming to design payloads in W-band for scientific experiments. Main research interests: Novel Air Interfaces for future wireless systems, in particular MIMO in Single carrier systems with Frequency Domain Equalization, EHF satellite communications, power control and resource management, UWB for biomedical applications.



Tommaso Rossi received the "Laurea" Degree in Telecommunications Engineering in 2002, MSc Degree in "Advanced Communications and Navigation Satellite Systems" in 2004 and Ph.D in Telecommunications and Microelectronics Engineering in 2008 from the University of Rome "Tor Vergata" where he is currently an Assistant Professor.



He is part of the scientific team that is defining ESA "TDP#5" (Technology Demonstration Payload, to be embarked on Alphasat satellite) telecommunication experiments. He has been a technical member of University of Rome "Tor Vergata" team working on projects funded by the Italian Space Agency: "FLORAD" project (2007/2008), as responsible for design, optimisation and analysis of a Flower Constellation of millimeter-wave radiometers for atmospheric observation; "WAVE" project (2004/2007), feasibility study for W-band satellite telecommunication payloads, as responsible for small-LEO mission definition and payload design activities; "TRANSPONDERS" project (2004/2008), feasibility study for Q/V-band satellite telecommunication payloads.

In 2007/2008 he has been involved in ESA "European Data-Relay Satellite System" project, as responsible for EDRS-user segment visibility analysis and Q/V-bands link budgets analysis. In 2006 he worked on ESA research project on "Flower Constellation Set and Its Possible Applications" as responsible for the design and

optimisation of Flower Constellations for communication, navigation and Earth/space observation applications. His research activity is focused on Space Systems, EHF (Extremely High Frequency) Satellite and Terrestrial Communications, Satellite and Inertial Navigation Systems, Digital Signal Processing and Satellite Constellations Design.

Asher Yahalom is an Associate Professor in the Faculty of Engineering at the Ariel University Center of Samaria and the Academic director of the free electron laser user center which is located within the University Center campus. He was born in Israel on November 15, 1968, received the B.Sc., M.Sc. and Ph.D. degrees in mathematics and physics from the Hebrew University in Jerusalem, Israel in 1990, 1991 and 1996 respectively. Asher Yahalom was a postdoctoral fellow (1998) in the department of electrical engineering of Tel-Aviv University, Israel. In 1999 he joined the faculty of the Ariel University Center of Samaria. During the years 2005-2006 he was a Senior Academic Visitor in the University of Cambridge, Cambridge, UK.



Yosef Pinhasi is a Professor in the Faculty of Engineering at Ariel University Center of Samaria. He received the B.Sc., M.Sc. and Ph.D. degrees in electrical engineering from Tel-Aviv University, Israel in 1983, 1989 and 1995 respectively. During the years 2003-2007, he served as the chairman of the Department of Electrical and Electronic Engineering, and is the head of the Institute of Technological Research for Defense and Homeland security. Since 1990 he is working in the field of electromagnetic radiation, investigating mechanisms of its excitation and generation in high power radiation sources like microwave and millimeter wave electron devices, free-electron lasers (FELs) and masers. Prof. Pinhasi is the head of many research projects granted by the Israeli Science foundation, Ministry of Infrastructure, Ministry of Industry and Commerce and Ministry of Defense. He published papers and articles in scientific journals, presented his work in national and international conferences and meetings and carries consultation works in communications to the industry and governmental ministries. He is author of 2 books. Prof. Pinhasi serves as the chairman of the Communication Technology and Smart Houses Chapter, the Society of Electrical and Electronic Engineers in Israel.



John Farserotu received the B.S.E.E. degree from the University of Maryland in 1983, the M.S.E.E. from George Washington University in 1985 and his Doctorate from the Delft University of Technology, The Netherlands in 1998. He is the Head of Wireless Program in the Integrated and Wireless Systems Division at CSEM.



Dr. Farserotu has authored or co-authored over 60 publications in major journals and conferences. He is co-author of a book on Mobile Satellite over IP/ATM Networks and he teaches a course on this subject at the Ecole Polytechnique Federale de Lausanne (EPFL). Dr. Farserotu is active in the IEEE802.15 Task Group 6 (BAN). He is Vice-Chair of ETSI eHealth and also Vice-Chair and Research Coordinator of the HERMES Partnership, a network of leading European R&D centers in the field of wireless and mobile communication. He is a member of the Editorial Board of the Springer Wireless Personal Communications journal, and has served on the program and organizing committees of major international conferences in wireless and mobile communication. From 1990 to 1998, he was with the NATO C3 Agency, The Hague, The Netherlands, where he was a Principal Engineer. Prior to that, he was a Senior Engineer/Manager at Stanford Telecommunications, Reston Va.

Claudio Sacchi obtained the “Laurea” Degree in Electronic Engineering, and the Ph.D. in Space Science and Engineering at the University of Genoa (Italy) in 1992 and 2003, respectively. Since August 2002, Dr. Sacchi has been holding a position as assistant professor at the Faculty of Engineering of the University of Trento (Italy). The research interests



of Dr. Sacchi are mainly focused on: broadband terrestrial and satellite transmission systems, MIMO systems, multi-rate and multi-access wireless communications, software-defined radio, etc. Claudio Sacchi is author and co-author of about 70 papers published in international journals and conferences. He is associate editor of IEEE COMMUNICATIONS LETTERS and reviewer for international journals and magazines. Claudio Sacchi is Senior Member of IEEE (SM'07), member of the IEEE Communications Society and of the IEEE AES Society.